

Dalton Transactions

Accepted Manuscript

This article can be cited before page numbers have been issued, to do this please use: Y. Deng, C. Hou, R. I. Walton, J. Tang, P. Zhu, K. Zhang and N. S. Weng, *Dalton Trans.*, 2013, DOI: 10.1039/C3DT51118A.



This is an *Accepted Manuscript*, which has been through the RSC Publishing peer review process and has been accepted for publication.

Accepted Manuscripts are published online shortly after acceptance, which is prior to technical editing, formatting and proof reading. This free service from RSC Publishing allows authors to make their results available to the community, in citable form, before publication of the edited article. This *Accepted Manuscript* will be replaced by the edited and formatted *Advance Article* as soon as this is available.

To cite this manuscript please use its permanent Digital Object Identifier (DOI®), which is identical for all formats of publication.

More information about *Accepted Manuscripts* can be found in the [Information for Authors](#).

Please note that technical editing may introduce minor changes to the text and/or graphics contained in the manuscript submitted by the author(s) which may alter content, and that the standard [Terms & Conditions](#) and the [ethical guidelines](#) that apply to the journal are still applicable. In no event shall the RSC be held responsible for any errors or omissions in these *Accepted Manuscript* manuscripts or any consequences arising from the use of any information contained in them.

Preparation, structural diversity and characterization of a family of Cd(II)-organic frameworks

Ye Deng,^[a] Chuan-Tao Hou,^[a] Richard I. Walton,^[b] Jiaqian Tang,^[a] Peizhi Zhu,^[a]
Kou-Lin Zhang,^{*[a,b]} Seik Weng Ng^[c]

^[a] College of Chemistry and Chemical Engineering, Yangzhou University, Yangzhou 225002, P.R. China

^[b] Department of Chemistry, University of Warwick, Coventry, CV4 7AL, UK

^[c] Department of Chemistry, University of Malaya, 50603, Kuala Lumpur, Malaysia

Two Cd(II)-organic frameworks based on 5-iodoisophthalate (IIP²⁻), {[Cd(IIP)(bte)(H₂O)]·H₂O}_n (**1**) and [Cd(IIP)(bpp)(H₂O)]_n (**2**), were obtained either at ambient temperature or under solvothermal condition at 120 °C in the presence of 1,4-bis(1,2,4-triazol-1-yl)ethane (bte) and 1,3-bis(4-pyridyl)propane (bpp) as auxiliary ligands, respectively. **1** is a novel discrete single-walled Cd(II)-organic tube (SWCOT) further extending into a 3D supramolecular interdigitated microporous columnar architecture supported by C-I...I halogen bonds and hydrogen bonds, while **2** exhibits an interesting two-fold interpenetrated 3D diamond network architecture. When the auxiliary ligands bte or bpp were replaced by a longer spacer ligand with more flexibility, 1,4-bis(triazol-1-ylmethyl)benzene (bbtz), the unique discrete single-walled Cd(II)-organic nanotube (SWCONT), {[Cd(IIP)(bbtz)(H₂O)]·H₂O}_n (**3**), which further extends into a 3D supramolecular microporous framework supported by face-to-face π...π stacking interactions and hydrogen bonds, was generated at room temperature. Under solvothermal condition at 120 °C, an interesting two-fold 2D “embracing” (4, 4) topological network, [Cd(IIP)(bbtz)(H₂O)] (**4**), which further

*Corresponding author. Tel /Fax: +86 514 87975244. E-mail: klzhang@yzu.edu.cn; koulinzhang2002@yahoo.com

extends into a two-fold 3D “embracing” supramolecular framework through O-H...O hydrogen bonds, is obtained. **4** loses crystallinity in air, leading to the formation of [Cd(IIIP)(bbtz)]·0.5H₂O (**4A**) evidenced by elemental analysis, thermographic analysis (TG) and powder X-ray diffraction pattern (PXRD). Remarkably, *in situ* rapid and reversible dehydration-rehydration under static air occurs in **1** - **3**, indicating their potential application as water absorbent and sensing materials. Dehydrated **1** and **3** show selective gas adsorption of CO₂ over N₂ and dehydrated **3** can adsorb methanol and ethanol vapors strongly. These compounds exhibit blue fluorescence in the solid state.

Introduction

Recently, the rational design and synthesis of metal-organic frameworks (MOFs) have created much interest due to the intriguing topologies of the materials and their potential applications in adsorption, catalysis and other technologies.¹⁻⁴ The architectures of MOFs depend on several factors, such as the chemical structure of the ligand, preferred coordination geometry of the metal ions and a number of experimental variables such as the solvent, temperature and templates, *etc.*⁵⁻¹⁰ Although carbon nanotubes have been intensively studied since their discovery in 1991,¹¹ only a few MOFs with nanotubular structure have as-yet been synthesized.¹² This may be because it is difficult to prepare discrete metal-organic nanotubes (MONTs) owing to the possibility of interlocks or interpenetration. Compared to 3D nanotubular MOFs, discrete MONTs may have different adsorption properties and even new applications in nanotechnology.¹³⁻¹⁴ Therefore, it is still a particularly

challenging subject to design and construct discrete MONTs.

From a design perspective, to assemble MOFs, the linking mode of the ligand should meet with the coordination geometry of the metal ion. Some specific strategies have been used to attempt to construct discrete MONTs. For instance, it has been reported that 0D squares can be connected from their four vertices by bridging organic ligands to generate novel interpenetrating or noninterpenetrating MONTs.^{13a,c} Previously, we performed a systematic study focusing on the temperature and auxiliary ligand-controlled assembly in a series of Zn(II)-organic frameworks based on 5-iodoisophthalic acid (H₂IIP) in the presence of btp as auxiliary ligand; we thus successfully obtained the first discrete single-walled Zn(II)-organic tube with dimensions of 0.92 × 0.90 nm² based on the 0D elliptical dimeric Zn(II) subunit.¹⁵ This gives us an indication that d¹⁰ metal ions when connected by flexible organic ligands with appropriate length and intramolecular interdigitated angle generate a nanosized elliptical dimeric unit, which then the rigid organic ligand links the elliptical subunits from the two vertexes to generate a discrete single-walled Cd(II)-organic nanotube (SWCONT) (**Chart 1**).

In this paper, we use H₂IIP as a rigid ligand and 1,4-bis(1,2,4-triazol-1-yl)ethane (bte), 1,3-bis(4-pyridyl)propane (bpp) and 1,4-bis(triazol-1-ylmethyl)benzene (bbtz) as auxiliary flexible ligands to assemble Cd(II) frameworks under different reaction conditions. Our strategy is based chiefly on the following considerations: (1) The iodide group is a potential interaction site for creating C-I...I/N/O halogen bonds which may help to extend the structure into a high-dimensional supramolecular

framework due to its specific directional nature and relatively high halogen bonding energy;¹⁶ and (2) The auxiliary flexible ligands chosen each has two different conformations: *T* (*trans*) and *G* (*gauche*) for bte,¹⁷ *TG* (*trans-gauche*) and *GG* (*gauche-gauche*) for bpp and bbtz,¹⁸ so their coordination modes may be influenced by the reaction conditions. The *G* conformation of bte and *GG* conformation of bpp and bbtz have the potential to form elliptical dimeric units with the d¹⁰ metal ion, which may further be connected by the rigid ligand IIP²⁻ leading to the formation of a discrete single-walled metal-organic tube. Thus, a structural prediction of the resulting framework may be possible to some extent.

Herein, a novel discrete single-walled Cd(II)-organic tube (SWCOT) {[Cd(IIP)(bte)(H₂O)]·H₂O}_n (**1**) and an interesting two-fold interpenetrated 3D framework with diamond topology [Cd(IIP)(bpp)(H₂O)]_n (**2**) were obtained with IIP²⁻ in the presence of bte and bpp, respectively (**Scheme 1**). When bte and bpp were replaced by a more flexible one with longer spacer, bbtz, a unique discrete single-walled Cd(II)-organic nanotube, {[Cd(IIP)(bbtz)(H₂O)]·H₂O}_n (**3**), and an interesting two-fold 2D “embracing” (4, 4) topological network, [Cd(IIP)(bbtz)(H₂O)] (**4**), were obtained at ambient temperature and under solvothermal condition at 120 °C, respectively. **4** loses crystallinity in the air and transforms into [Cd(IIP)(bbtz)]·0.5H₂O (**4A**). Thermal stability and solid state fluorescent properties of **1-3** and **4A** have been studied. Dehydration-rehydration behavior of **1-3** had been investigated. The gas and vapor adsorption of **1** and **3** had also been performed.

Results and discussion

Synthesis of the complexes

The discrete SWCOT **1** as well as the two fold interpenetrated 3D diamond topological network **2** could be obtained at either room temperature or under solvothermal condition at 120 °C, while at these two corresponding temperatures, a pair of temperature-dependent frameworks, the discrete SWCONT **3** and **4**, were obtained. Interestingly, the molar ratio of H₂IIP:NaOH is very important for the growth of single crystals. During the synthesis of **1** and **2**, the molar ratio of H₂IIP:NaOH (1:0 for **1** and 1:2 for **2**) was used at room temperature, while the molar ratio of H₂IIP:NaOH (1:0.5 for **1** and 1:1 for **2**) was used under solvothermal condition at 120 °C although the synthesis of both **1** and **2** is temperature-independent. At the higher temperature, however, polycrystals or cotton-like solids were obtained. The molar ratio of H₂IIP:NaOH (1:2) was used in attempts to synthesize **3** and **4**. It should be noted that **3** and **4** were not obtained without the presence of small quantities of *N*, *N'*-dimethylformamide (DMF) and ethanol, respectively. This indicates that the cosolvent has great influence on the crystal growth of these MOFs. There are great differences in the coordination modes of the auxiliary ligand bbtz (**Scheme 1**), which exert an important influence on the crystalline architectures of **3** and **4** as described below.

Structural description of the tube {[Cd(IIP)(bte)(H₂O)]·H₂O}_n (**1**)

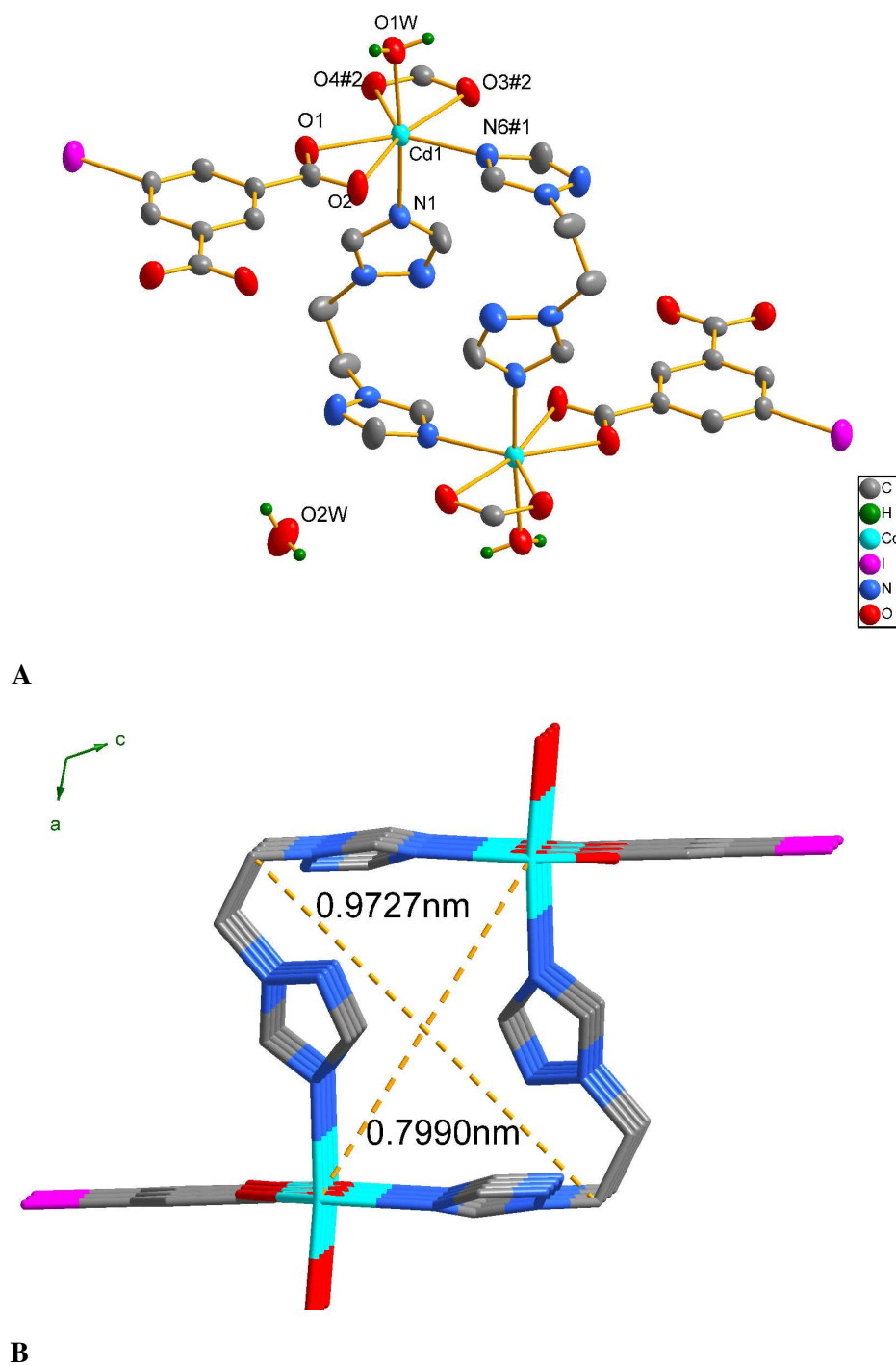
The SWCOT **1** crystallizes in the monoclinic system with space group *C2/c* and exhibits a novel 1D single-walled tubular chain structure. The asymmetric unit contains one Cd(II) ion, one IIP²⁻ anion, one bte ligand, one coordinated water and

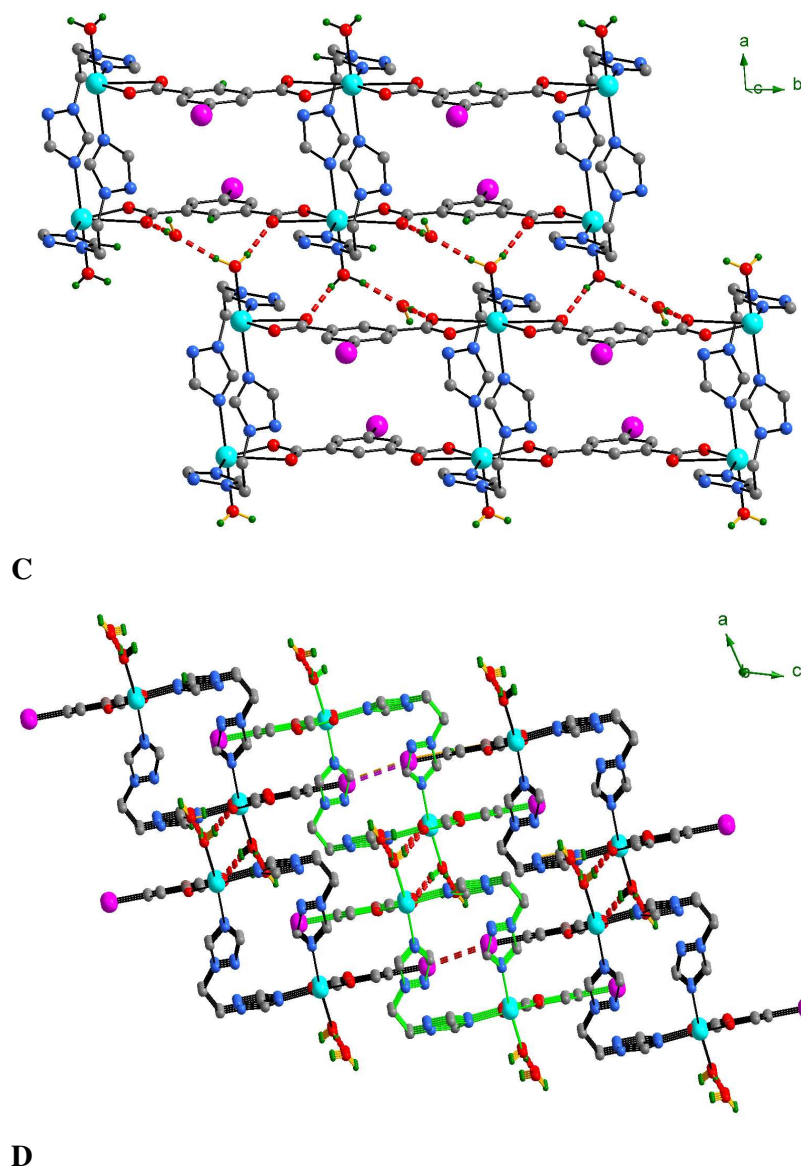
one lattice water molecule. The central Cd(II) ion is heptacoordinated by four carboxylate oxygen atoms from two different IIP²⁻ ligands, two nitrogen atoms from two different bte ligands and one water molecule in a pentabipyramidal coordination geometry with average Cd–O_{carboxylate} and Cd–N_{bte} distances of 1.952 Å and 2.008 Å, respectively (**Fig. 1A**, **Table 1**). The auxiliary flexible ligand bte acts as a bidentate bridging ligand showing a *G(gauche)* conformation (**Scheme 1**) with a dihedral angle of 65.17° between the two triazole rings and intramolecular N1...N6 distance of 5.169 Å, linking the Cd(II) nodes into an elliptical dimeric unit [Cd(bte)₂Cd]. The dimeric subunits [Cd(bte)₂Cd] are further connected by the main rigid ligand IIP²⁻ with the (κ²)-(κ²)-μ₂ bridging mode to generate a novel discrete single-walled tube with the dimensions of 0.9727 × 0.7990 nm² along [010] direction (**Fig. 1B**). The nearest intrachain Cd...Cd distance separated by the IIP²⁻ bridge is 10.461 Å and the interstitial water molecules are situated close to the wall of the tube.

If water molecules are ignored, calculations with the SQUEEZE program from the PWT¹⁹ show that, in the evacuated regions of SWCOT **1**, the available volume for the inclusion is 299.3 Å³ per cell unit, *i.e.* 7.7 % of the crystal volume of 3865.0 Å³.

Both the coordinated and lattice water molecules form a water dimer. The intertubular hydrogen bonds further extend the discrete tube into 2D supramolecular layer [O1W-H1WA...O4 2.790(9), O1W-H1WB...N2 3.010(11), O2W-H2WA...O2 2.891(7) and O2W-H2WB...O3 3.007(8) Å] (**Fig. 1C**, **Table 2**). The lattice water O2W acts as hydrogen bond donor and acceptor, while the coordinated water molecule O1W serves as double hydrogen bond donor. Interestingly, 2D

supramolecular layer interpenetrates each other through the halogen bond C-I...I (3.791 Å), resulting in the formation of a 3D supramolecular microporous interdigitated columnar network (**Fig. 1D**).





D

Fig. 1 A The coordination environment of Cd(II) and the conformation of btp in **1**. (Symmetry codes: #1 $-x+2, -y, -z+1$ #2 $x, y-1, z$).

B Ball and stick representation of 1D tube along [010] direction with internal dimensions.

C 2D supramolecular layer, showing the coordination mode of IIP²⁻ and the hydrogen bonding pattern (red dotted lines).

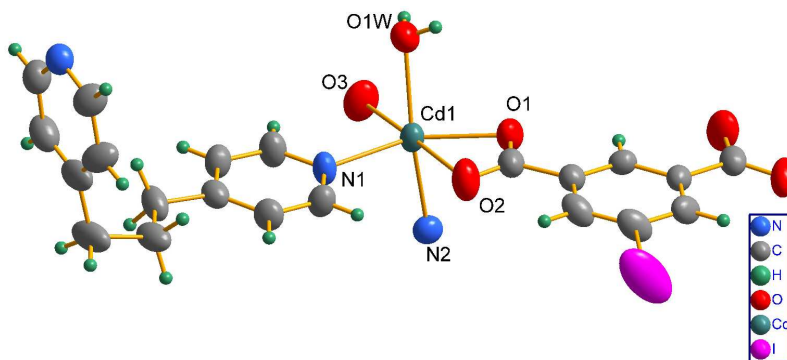
D 2D supramolecular layer interpenetrates each other through the halogen bond C-I...I (pink dotted lines), resulting in a 3D supramolecular microporous framework.

Structural description of crystalline polymer $[Cd(IIP)(btp)(H_2O)]_n$ (**2**).

Single crystal X-ray structural analysis shows that **2** crystallizes in the monoclinic system with space group $C2/c$ and exhibits a two-fold interpenetrated 3D diamond network architecture. The asymmetric unit consists of one Cd(II) ion, one IIP²⁻, one

bpp ligand and one coordinated water. Each six-coordinated Cd(II) ion is bound by two N atoms from two bpp ligands, four oxygen atoms from two IIP²⁻ ligands and coordinated water, which exhibits a distorted octahedral coordination geometry with the subtended angles ranging from 52.65(12) to 175.77(13)° (**Fig. 2A, Table 2**). One of the carboxylate groups in the IIP²⁻ ligand exhibits the monodentate bridging conformation, while the other one exhibits the chelating coordination mode, So the IIP²⁻ ligand adopts the (*k*¹)-(*k*²)- μ_2 coordination mode to connect the adjacent Cd(II) ions into a zigzag-like double chain along [100] direction (**Fig. 2B**). These chains are further connected by bpp ligands in *TG*(*trans-gauche*) conformation (**Scheme 1**), leading to the formation of 3D architecture.

If the Cd(II) ions are treated as nodes, both the IIP²⁻ and bpp ligands as linkers, the framework of **2** can be viewed as a two-fold interpenetrated 3D diamond network, which are further connected with each other through $\pi \dots \pi$ [(3.711(2) Å] stacking and C-H... π interactions [H...pyridyl centroid: 2.954(2) Å] (**Fig. 2 C-D**).



A

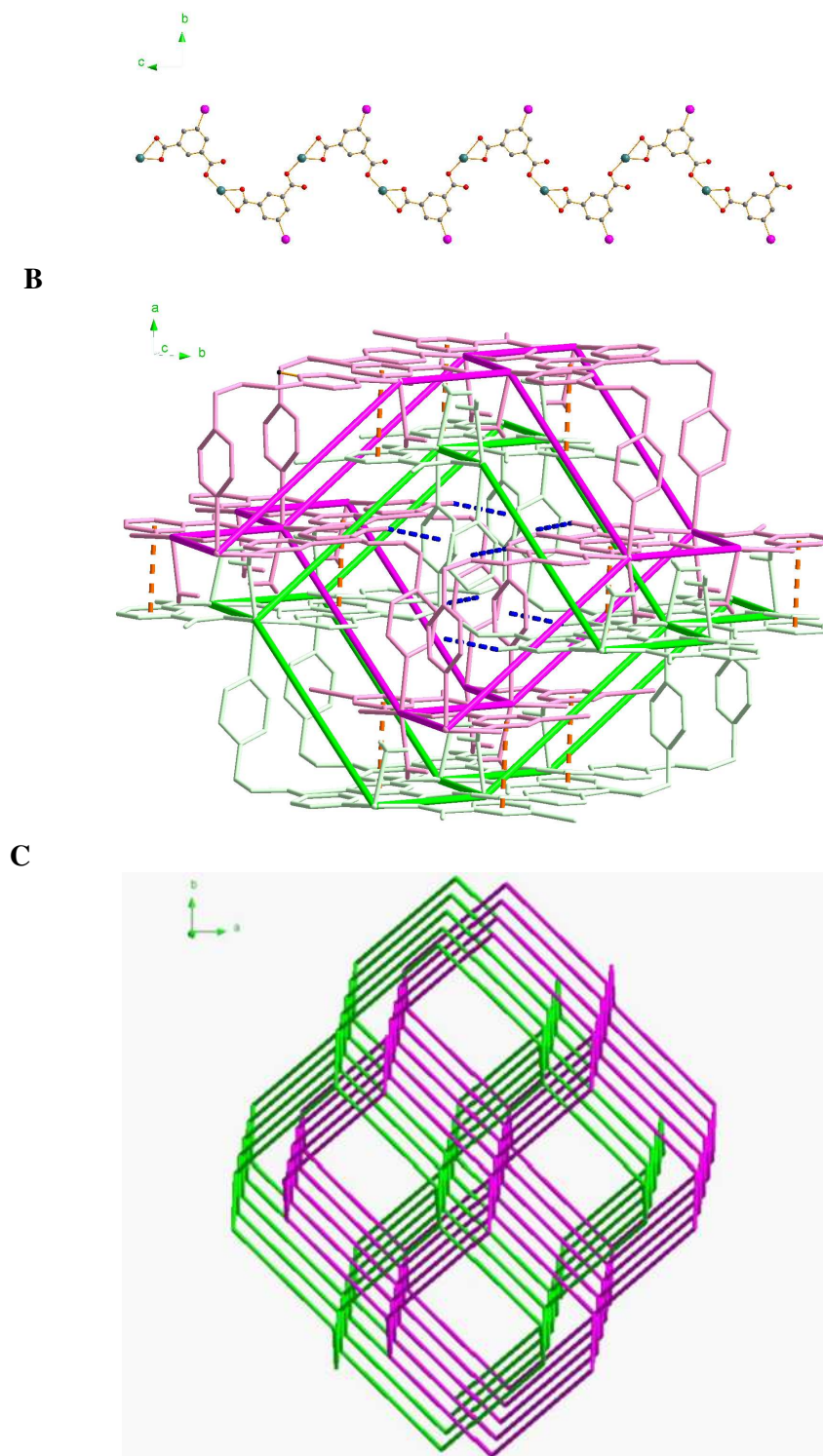


Fig. 2 **A** View of the coordination environment of Cd(II) in **2** ($\#5$ $x, 1-y, 1/2+z$ $\#6$ $-1/2+x, 1/2-y, -1/2+z$).

B View of the 1D carboxylate-bridged zigzag chain in **2** along c axis.

C View of the two-fold interpenetrated 3D nets connected with each other through $\pi \dots \pi$ stacking and C-H... π interactions (blue dashed lines).

D Schematic drawing of the two-fold interpenetrated diamond network.

Structural description of the nanotube $\{[\text{Cd}(\text{IIP})(\text{bbtz})(\text{H}_2\text{O})]\cdot\text{H}_2\text{O}\}_n$ (**3**)

Replacement of the auxiliary ligands bte and bpp by a more flexible ligand with longer spacer length, bbtz, yielded the novel discrete Cd(II)-organic nanotube **3** which was obtained at room temperature. Different from **1**, compound **3** crystallizes in the triclinic system with space group *P*-1 and has a novel discrete nanotubular chain structure. The central Cd(II) atom adopts the pentagonal bipyramidal coordination geometry through bonding to four O-donors from two IIP²⁻ ligands, two triazole N-donors from two bbtz ligands and one O-donor from the coordinated water molecule (**Fig. 3A, Table 2**).

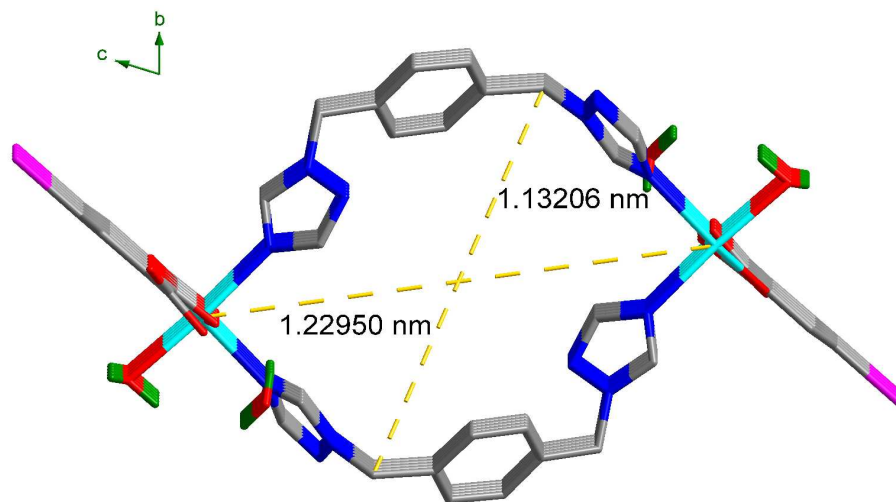
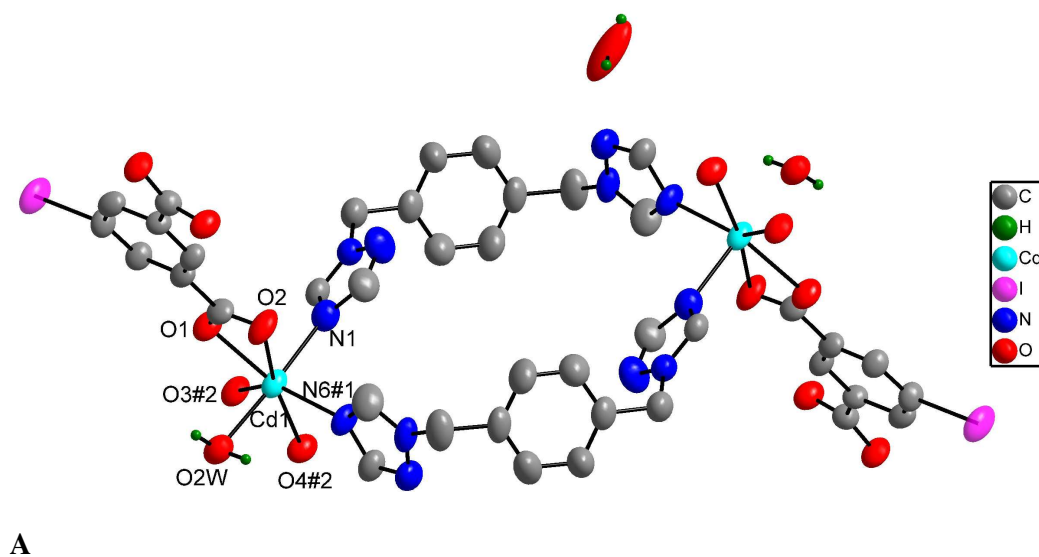
As expected, two bbtz ligands coordinate to two Cd(II) atoms to form an nanosized elliptical dimeric metallamacrocyclic ring $[\text{Cd}(\text{bbtz})_2\text{Cd}]$ in which the auxiliary flexible ligand bbtz adopts *GG(gauche-gauche)* conformation (**Scheme 1**). Compared with bte in SWCOT **1**, the auxiliary ligand bbtz in SWCONT **3** has a bigger bent angle between two triazole rings (67.47°) and a longer intramolecular N1...N6 distance [$9.2159(12) \text{ \AA}$], which are mainly responsible for the formation of nanosized elliptical dimeric subunit. The elliptical dimeric rings thus created are then further linked with each other through the rigid IIP²⁻ ligand in $(k^2)-(k^2)-\mu_2$ fashion to form a novel discrete single-walled elliptical nanotube (**Fig. 3B**). The nanotube lies parallel to the crystallographic *a*-axis and has an internal dimension of $1.22950 \times 1.13206 \text{ nm}^2$.

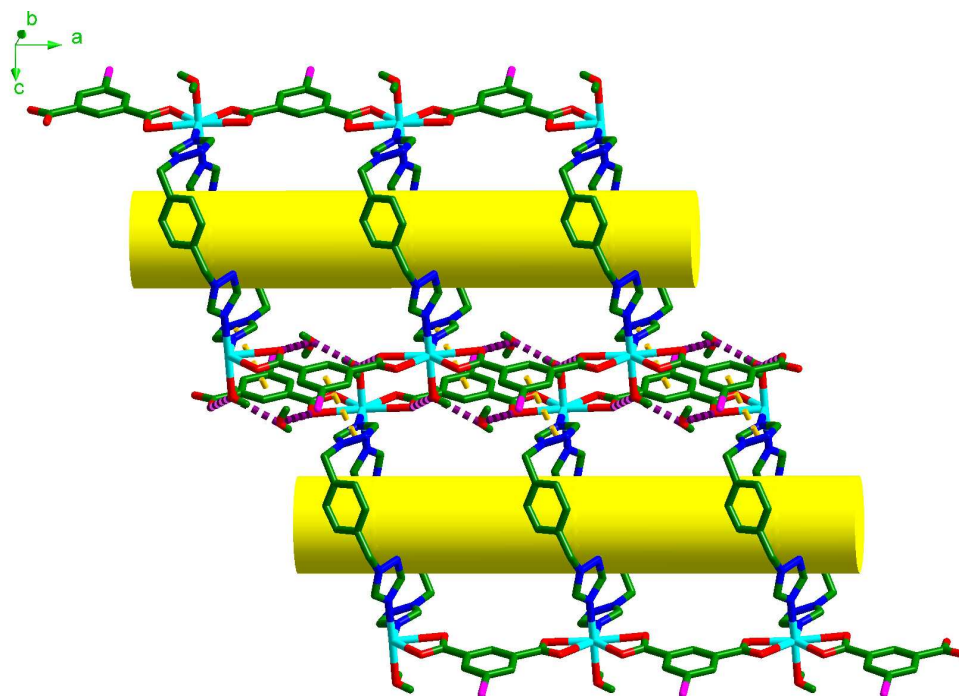
Quite different from SWCOT **1**, there are large solvent-accessible voids in SWCONT **3**. Calculations with the SQUEEZE program from PWT¹⁹ show that the

total solvent-accessible volume of **3** is 339.0 Å³ per unit cell, even including both the lattice water and coordinated water molecules, comprising 23.7 % of the crystal volume (1432.64 Å³). While in the structure of SWCOT **1**, there are no solvent-accessible voids if both the coordinated and lattice water molecules are included. If both the lattice water and coordinated water molecules are excluded, the total solvent-accessible volume in SWCONT **3** reaches 410.6 Å³ per unit cell, comprising 28.7 % of the crystal volume, which is quite larger than that in SWCOT **1**. This may result in its distinct adsorption/desorption properties to the guest molecules as described below.

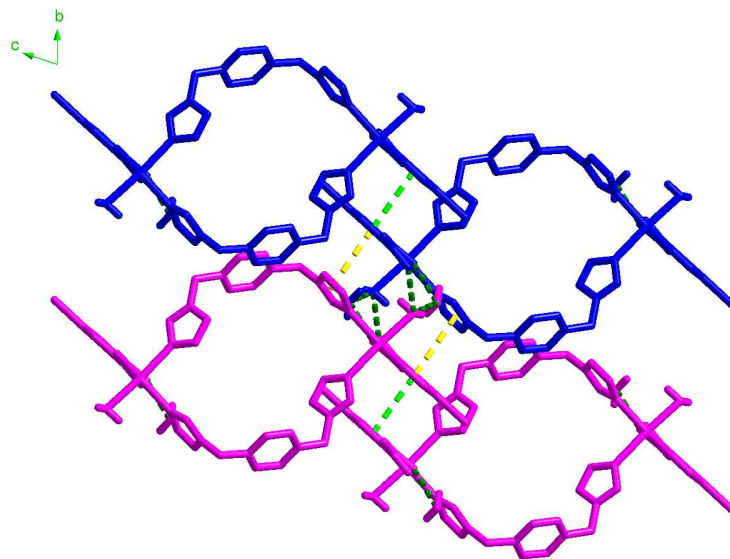
Similar to SWCOT **1**, in the proximity of the wall of SWCONT **3** is situated one ordered interstitial H₂O molecule. Both the interstitial water molecule and the coordinated one are organized into a discrete water dimer. The Ow...Ow distance [2.709(14) Å] is comparable to that for the ice II phase (2.77-2.84 Å).²⁰ The O1W and O2W are also hydrogen-bonded to both the coordinated and uncoordinated carboxylate oxygen atoms of the neighboring nanotubes by O1W-H1WA...O2 [2.714(17) Å] and O2W-H2WA...O4 [2.682(11) Å] (**Fig. 3C**). Thus, the nanotubes are aligned into a 2D columnar sheet driven by such O-H...O hydrogen bonds and face to face π...π stacking interactions between the benzene and triazole rings of the adjacent tubes [the centroid...centroid distance: 3.7216(4) Å]. The 2D supramolecular layer is further linked through face-to-face π...π stacking interactions between two benzene rings of the adjacent nanotubes with the centroid...centroid distance of 3.8970(4) Å, ultimately resulting in a 3D supramolecular microporous assembly

without interpenetration (**Fig. 3D**), which is quite different from the packing of SWCOT **1**.

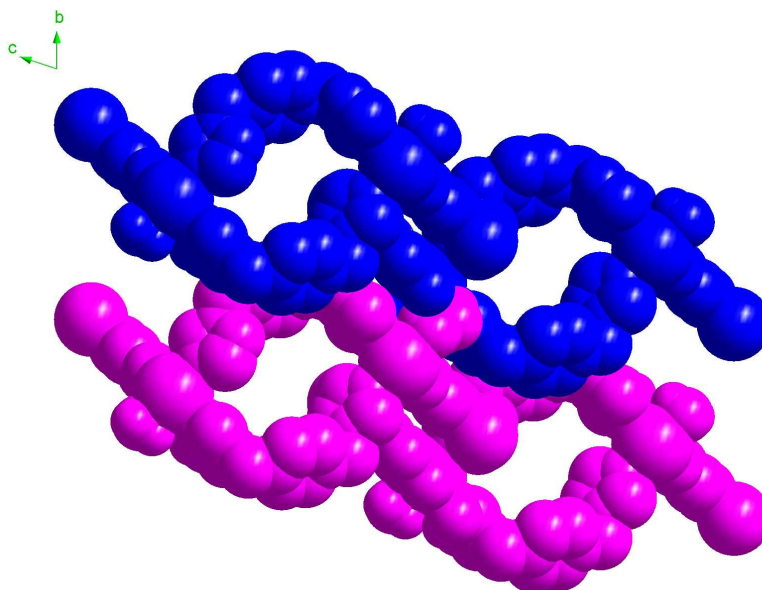




C



(Top)



(Bottom)

D

Fig. 3 A The coordination environment of Cd(II) and the elliptical dimeric metallamacrocyclic ring in **3**. (Symmetry codes: #1 1-x, -y, 1-z #2 x-1, y, z).

B 1D discrete single-walled nanotube, showing the lattice water molecules reside just in the wall of the tube.

C Supramolecular columnar layer formed through O-H...O hydrogen bonds and face to face π ... π stacking interactions.

D 3D supramolecular microporous framework without interpenetration, including both the coordinated and lattice water molecules.

Top: Stick representation;

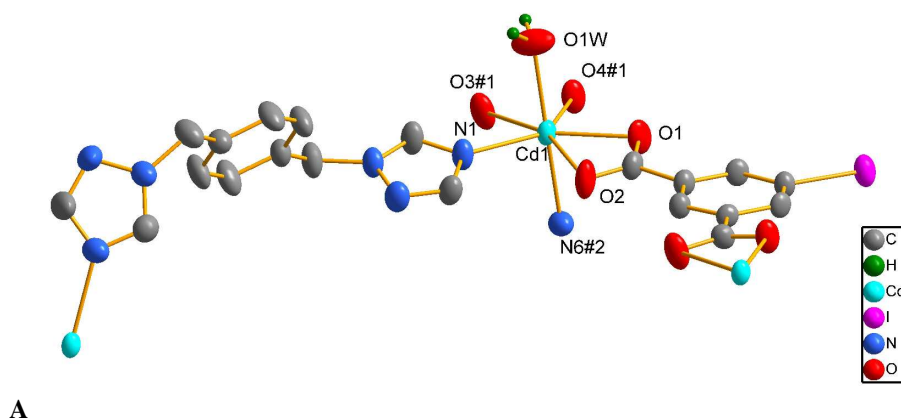
Bottom: Space filling diagram, showing the larger cavities within the nanotube.

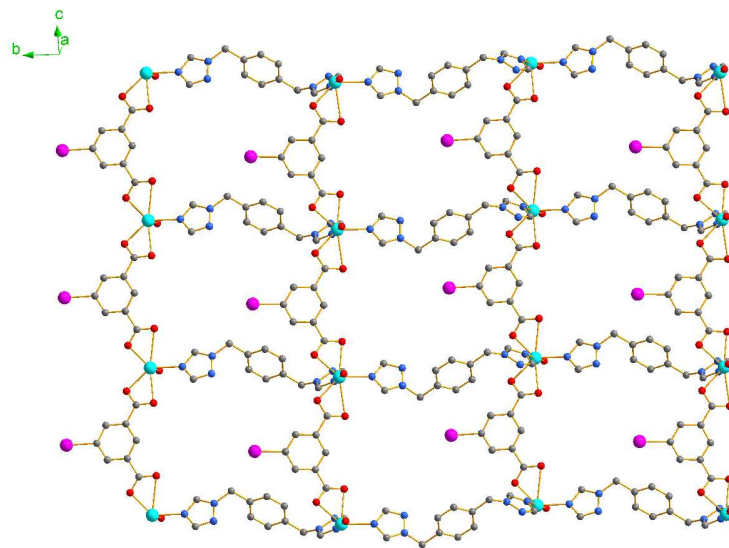
Structural description of the framework $[\text{Cd}(\text{IIP})(\text{bbtz})(\text{H}_2\text{O})]_n$ (**4**)

When the reaction used to prepare compound **3** was performed under solvothermal condition at 120 °C, an interesting 2D framework **4** was obtained. Compound **4** crystallizes in the monoclinic system with space group $P2_1/c$. The asymmetric unit of **4** contains one Cd(II) ion, one IIP²⁻ ligand, one bbtz ligand and one coordinated water molecule. The Cd(II) ion is heptacoordinated by four carboxylate oxygen atoms from two IIP²⁻ ligands, two nitrogen atoms from two bbtz ligands and one water molecule, resulting in a pentabipyramidal coordination geometry (**Fig. 4A**). The bbtz ligand

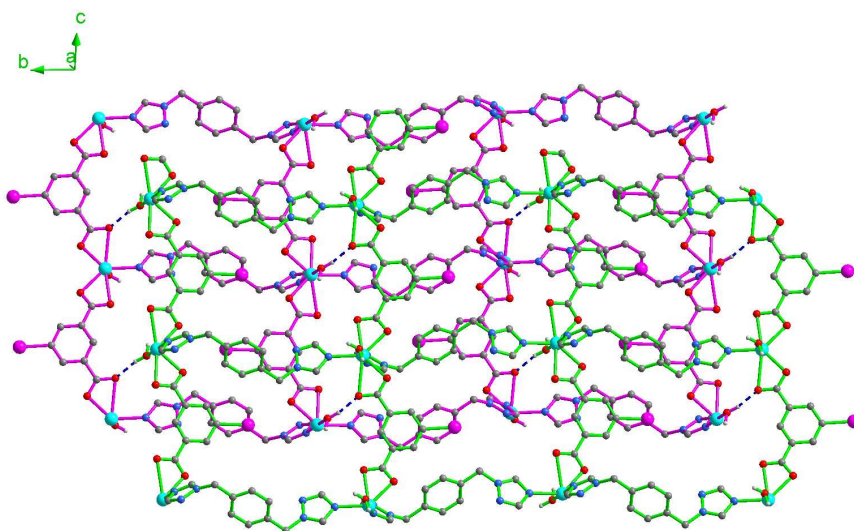
links the adjacent Cd(II) nodes to yield a 1D *zigzag* chain, which is further linked by the IIP^{2-} ligands to form a 2D (4, 4) topological net along [100] direction (**Fig. 4B**). The two carboxylate groups of IIP^{2-} ligand adopt the same chelating bidentate coordination mode, while the bbtz ligand adopts *TG(trans-gauche)* conformation (**Scheme 1**).¹⁸ Thus, 4-membered macrometalcyclic rings with dimensions of $12.820 \times 10.253 \text{ \AA}^2$ are formed.

The 2D (4, 4) topological net is further connected through the hydrogen bonds $\text{O1W} - \text{H1WA} \dots \text{O3} \ 2.746(4) \text{ \AA}$ and $\text{O1W} - \text{H1WB} \dots \text{N5} \ 2.848(6) \text{ \AA}$, leading to the formation of a 2D supramolecular “embracing” double-layer (**Fig. 4C**). These double arrays are further extended into a two fold 3D “embracing” supramolecular architecture *via* O-H...O hydrogen bonds (see **Table 3**) (**Fig. 4D**).

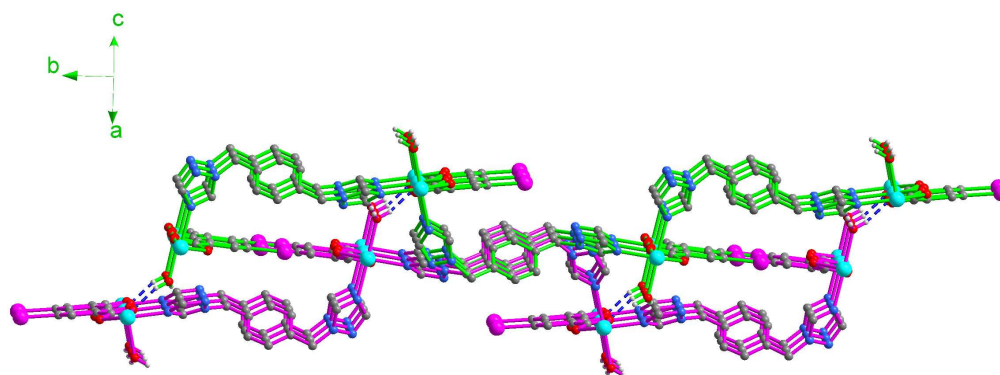




B

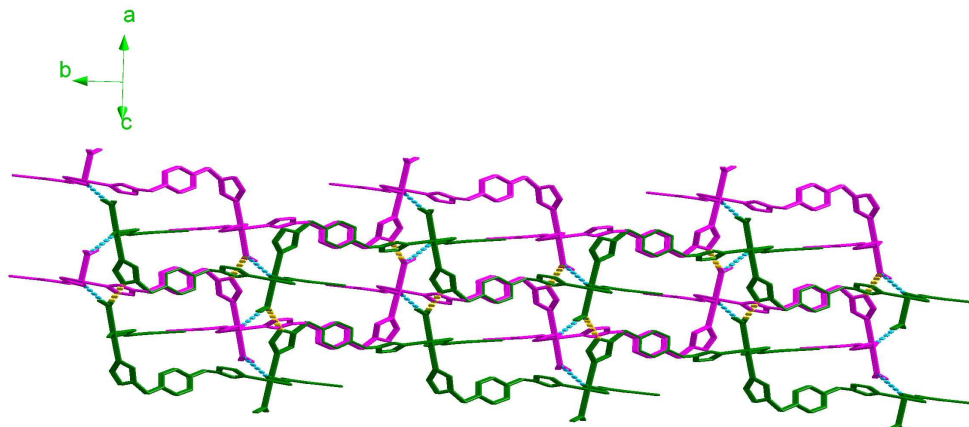


Top



Bottom

C



D

Fig. 4 A View of the Cd(II) coordination environment and the conformation of the bbtz ligand in **4**.

Symmetry code: #1 $x-1, y, z-1$ #2 $-x+2, y+1/2, -z+1/2$.

B 2D (4, 4) topological net.

C The adjacent 2D (4, 4) nets embrace with each other through hydrogen bonds, leading to the formation of 2D supramolecular double layer.

Top: View along $[-8.90, 2.65, 6.20]$; **Bottom:** Side view along $[-3.41, 0.41, -6.85]$ direction.

D Two-fold 3D “embraced” supramolecular framework through hydrogen bonds.

FT-IR spectra and thermal Stability

The FT-IR spectral data show features attributable to the carboxylate stretching vibrations of **1-3** and **4A**. The absence of bands in the range of $1680-1760\text{ cm}^{-1}$ indicates the complete deprotonation of H_2IIP in these four complexes. The characteristic bands of the carboxylate groups appear in the range $1552-1598\text{ cm}^{-1}$ for the asymmetric stretching and $1384-1490\text{ cm}^{-1}$ for the symmetric stretching, respectively. The broad band at 3120 cm^{-1} corresponds to the vibration of the water molecules in **1-3** and **4A**.²¹

To study the thermal stability of the compounds, thermogravimetric analysis (TGA) was performed on all samples under a nitrogen atmosphere in flowing N_2 with a heating rate of $10\text{ }^\circ\text{C}\cdot\text{min}^{-1}$ (**Fig. 4**). TGA of **1** suggests that the release of the water

molecules begins at about 67 °C. The total weight loss of 5.90 % up to 153 °C corresponds to the loss of both the coordinated water and lattice water molecules (calcd. 5.98 %).

For **2**, the first step weight loss of 2.56 % (calcd. 2.91 %) from 111 to 170 °C corresponds to the removal of one coordinated water molecule.

For **3**, the first step weight loss of 4.76 % (calcd. 5.30 %) in the temperature range 20 to 85 °C corresponds to the removal of two water molecules.

The weight loss of 0.84 % from 53 to 80 °C corresponds to the release of water molecule, which further reveals that the formula of the partly dehydrated phase of [Cd(IIP)(bbtz)(H₂O)]_n (**4**) is [Cd(IIP)(bbtz)]·0.5H₂O (**4A**) (calcd. 1.38 %). The second step begins from 240 °C and the whole decomposition process is complete at 800 °C. X-ray powder diffraction measurement further shows that the structure of **4A** is different from that of **4** (Fig. 5).

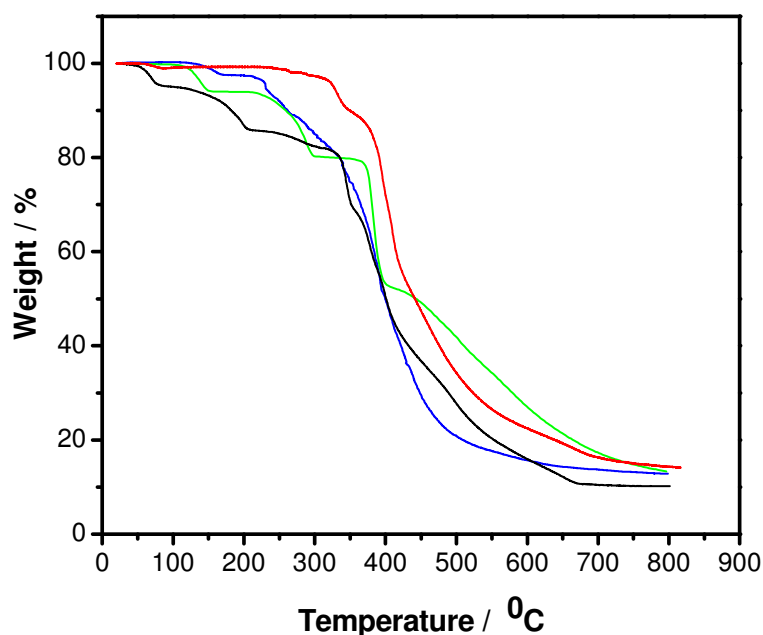


Fig. 4 TG curves of **1** (green), **2** (blue), **3** (black) and **4A** (red).

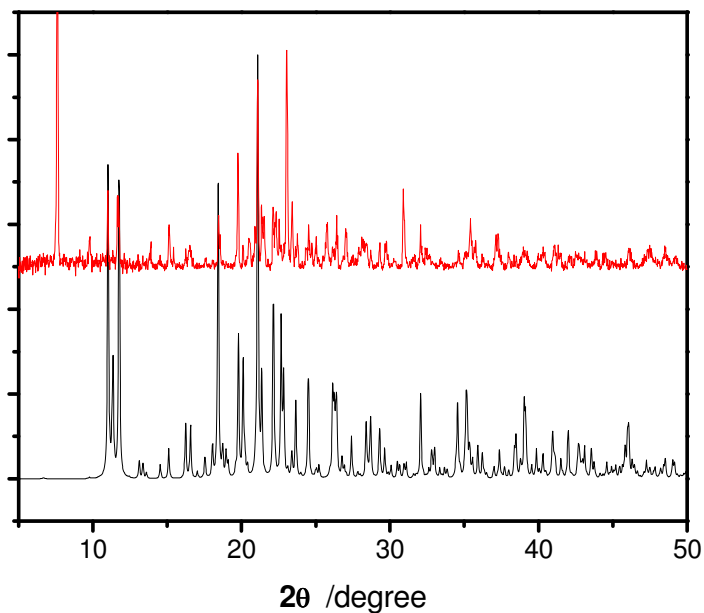


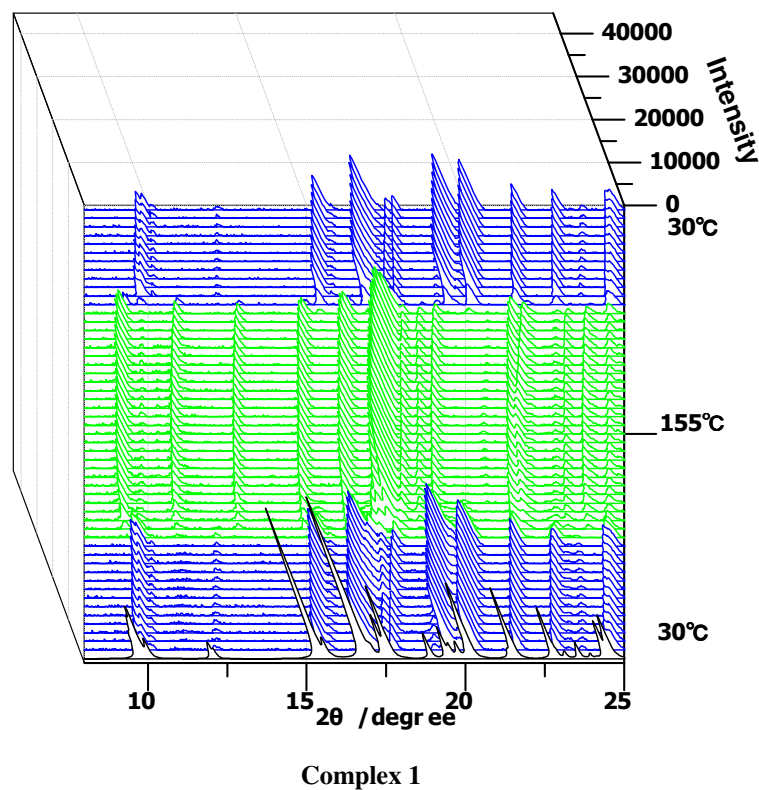
Fig. 5 PXRD patterns: (black) simulated from the single-crystal data of **4**, (red) for the powder sample **4A**.

Dehydration-rehydration properties of **1-3**

Thermogravimetric analyses (TGA) show clearly that both the interstitial and coordinated water molecules in **1-3** could be excluded upon heating. To study the dehydration-rehydration properties of **1-3**, the *in situ* variable temperature PXRD was performed on **1-3** over the temperature range 30-155 °C for **1**, 30-170 °C for **2** and 30-85 °C for **3**, respectively, in static air (**Fig. 6-8**). Remarkably, the PXRD patterns clearly show that **1-3** undergo reversible dehydration and rehydration; upon exposure of the dehydrated material in the static air, the dehydrated phase rehydrates rapidly, resulting in the re-establishment of the original crystal structure. This is further verified by the TG analysis of the rehydrated material of **1-3** [the first step mass loss corresponding to water molecules in TGA: 5.81 % (calcd. 5.98 %) for **1**, 2.88 % (calcd. 2.91 %) for **2** and 5.34 % (calcd. 5.30 %) for **3** (see **Fig. S1**)]. It should be pointed out that the dehydrated phases of **1-3** still remain integrity after the water

molecules are lost, but the structure of the desolvated materials are changed, as supported by the *in-situ* variable temperature powder X-ray diffraction (PXRD) patterns. This observation clearly indicates that during the process of dehydration and rehydration in **1-3** the frameworks exhibit a “breathing” property which may mainly be attributed to the flexibility of the auxiliary ligands bte, bpp and bbtz in the corresponding frameworks **1-3** since the main ligand IIP²⁻ is rigid.

The framework integrity of **1-3** can be maintained after a number of desorption/adsorption cycles, which indicate that **1-3** may be used as potential novel adsorbent as well as sensing materials to water molecules.



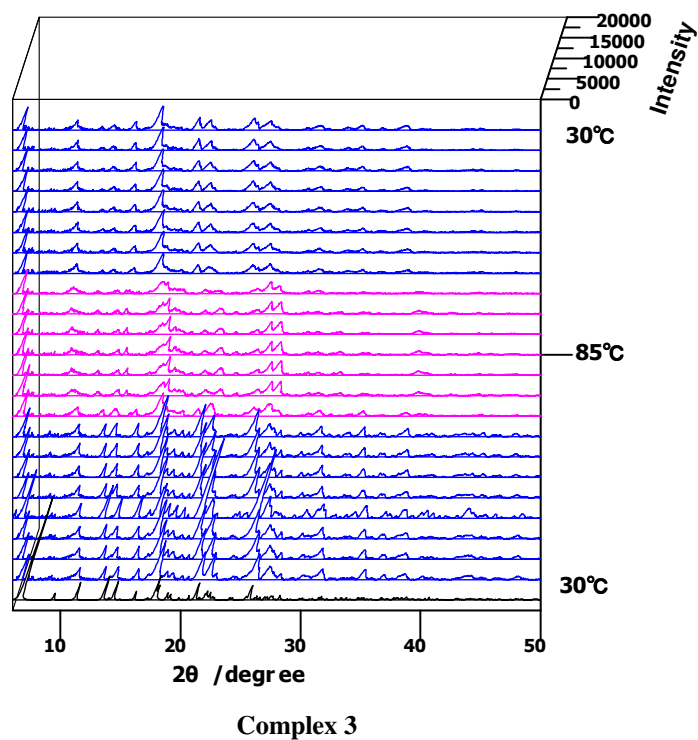
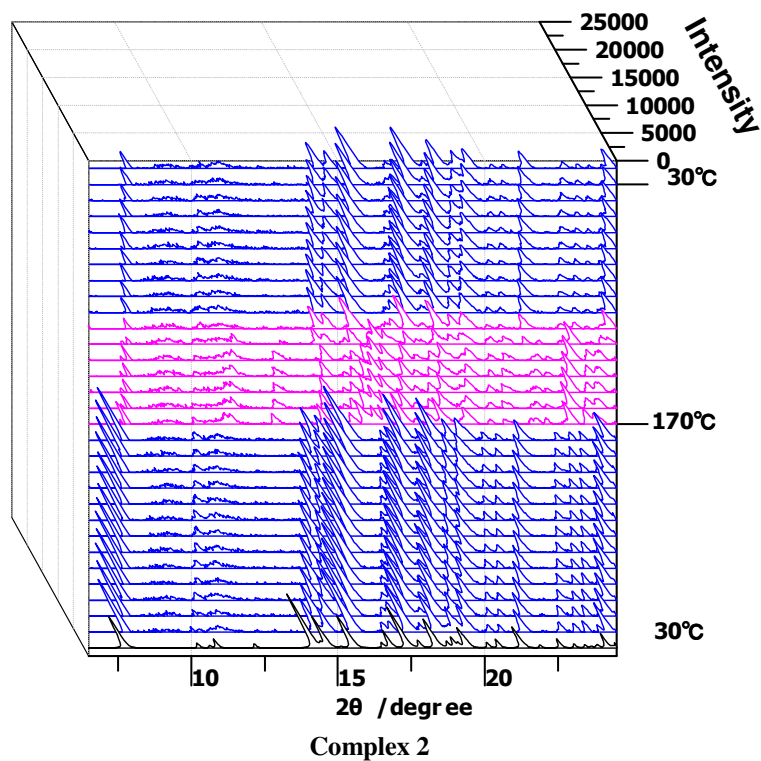


Fig. 6 VT-XRPD patterns recorded during the heating of **1-3** showing the complete departure of the water molecules at 155 °C (green line) for **1**, 170 °C (red line) for **2**, and 85 °C (red line) for **3**, leading to a new dehydrated phase which further shows rapid *in situ* reversible rehydration just in the static air. [(Black) the simulated XRPD patterns calculated from single-crystal data of **1-3** with Mercury 1.4.2.]

Desorption/adsorption to gas/vapors.

In order to test the ability of both the dehydrated SWCOT **1** and SWCONT **3** to host molecules other than water, several sorption experiments were carried out. For such a purpose, we considered molecules that exhibit current interest for storage, for example, carbon dioxide (CO₂) and nitrogen (N₂). Further, gas sorptions were performed at 278 K, to give more reliable results related to crystal structures determined at room temperature. The N₂ adsorption isotherm of the dehydrated **1** and **3** showed almost no uptake capacity. The gas sorption behavior of the dehydrated **1** and **3** showed distinct behavior in CO₂ uptake when compared to other MOFs reported in the literature (**Fig. 8**). Furthermore, the CO₂ adsorption isotherm of the dehydrated **1** and **2** showed quite different behavior with each other. For the dehydrated **1**, a significant hysteresis loop was observed. Above 20 atm, a large increase in gas sorption is observed, resulting in a final uptake of 65 mg.g⁻¹ (6.5 wt %) at 38 atm. In addition, the desorption isotherm also displayed one phase transition at 10 bar. The dramatic change in gas sorption behavior indicates the framework undergoes a phase change.²² But, the dehydrated **3** uptakes a relative lower amount of CO₂ (21 mg.g⁻¹; 2.1 wt %) at 38 bar, which may be due to the size of the resulting channel of **1** is much closer to the kinetic diameter of carbon dioxide (3.3 Å) than that of **3**. Quite different from that of the dehydrated **1**, no dramatic change in gas sorption was observed during both desorption and adsorption process, indicative of no phase transition occurring in the process. Overall, both the dehydrated **1** and **3** showed selective uptake of CO₂ over N₂ at 278 K under high pressure. The selective sorption

of CO₂ over N₂ gases may be attributed to both the smaller kinetic diameters of CO₂ compared to that of N₂ (CO₂, 3.3; N₂, 3.6 Å) and the significant quadrupole moment of CO₂ (-1.4×10^{-39} cm²), which generates specific interactions with the host framework.²³

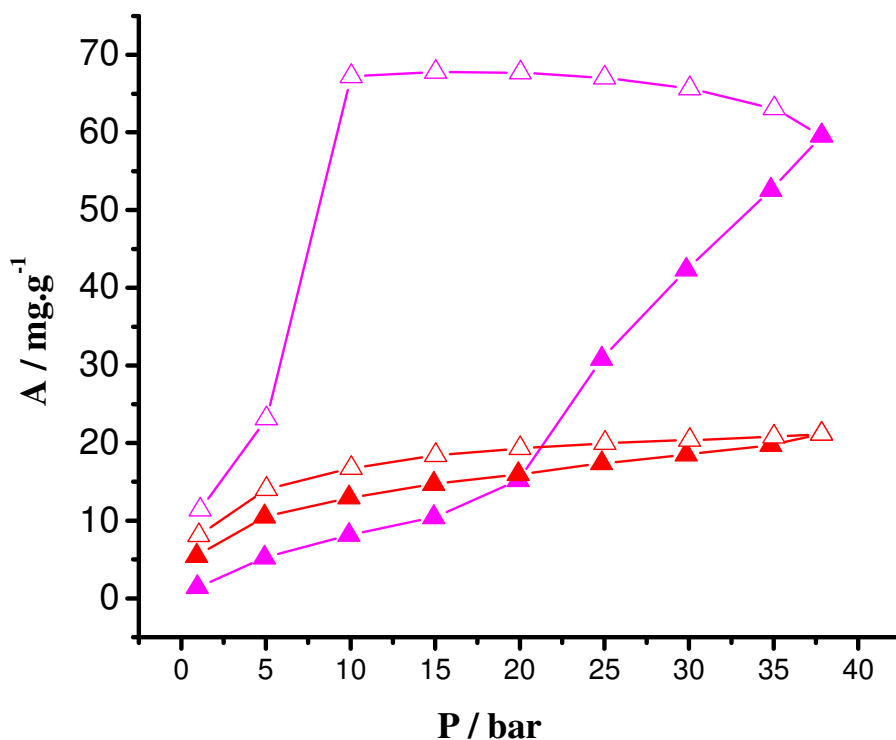


Fig. 8 Sorption isotherms of CO₂ measured at 278 K (1: pink; 3: red).

In addition, the dehydrated SWCOT **1** and SWCONT **3** were also subjected to some protic and aprotic solvent vapor adsorption, such as methanol, ethanol and acetone vapors. The adsorption to vapors was measured at 298 K. For the dehydrated **1**, the amounts adsorbed for these three corresponding vapors are 16.5, 7.8 and 3.6 mg·g⁻¹, respectively, while the dehydrated **3** showed much stronger adsorptions to these three corresponding vapors, which are 61.1, 93.2 and 16.8 mg·g⁻¹ (P/P₀: 0.73 for

methanol; 0.62 for ethanol and 0.72 for acetone), respectively. That the dehydrated **1** and **3** can adsorb methanol and ethanol vapor more strongly than acetone may be attributed to the fact that the protic polar solvents can form hydrogen bonds with the host tube. Furthermore, the strong adsorption ability to methanol and ethanol vapors of the dehydrated **3** reveals that the dehydrated **3** may be used as effective adsorbent material to some protic polar solvents.

Fluorescent properties

To well compare the relative fluorescent intensities of **1-3**, **4A** and free acid H₂IIP, we determined all the emission spectra with the same excitation wavelength. Excitation of the samples **1-3** and **4A** at 290 nm leads to the generation of similar blue fluorescent emissions with the maximum emission centered on 472 nm and a shoulder at about 412 nm (Fig. 9). To further understand the origin of these emission bands, the fluorescent spectrum of free H₂IIP acid has also been measured. The free H₂IIP acid exhibits the same maximum fluorescent emission and shoulder ($\lambda_{\text{ex}} = 290 \text{ nm}$) as those in **1-3** and **4A**. These observations suggest that the coordination of the IIP²⁻ ligand with Cd(II) ion in the presence of bte, bpp or bbtz as auxiliary ligands has no influence on the emission mechanism of the Cd(II)-organic frameworks.²⁴ So, the emissions of these three complexes may be assigned to an intraligand $\pi \dots \pi^*$ transition.²⁵ The strongest fluorescent intensity of **4A** compared with those of **1-3** may be attributed that **4A** has the least lattice water molecules among the three complexes. The enhancement of fluorescence in the complexes **1-3** and **4A** may be attributed to the ligation of the ligand to the metal center, which further enhances the rigidity of the

ligand IIP^{2-} and reduces the loss of energy through a radiationless pathway.²⁸

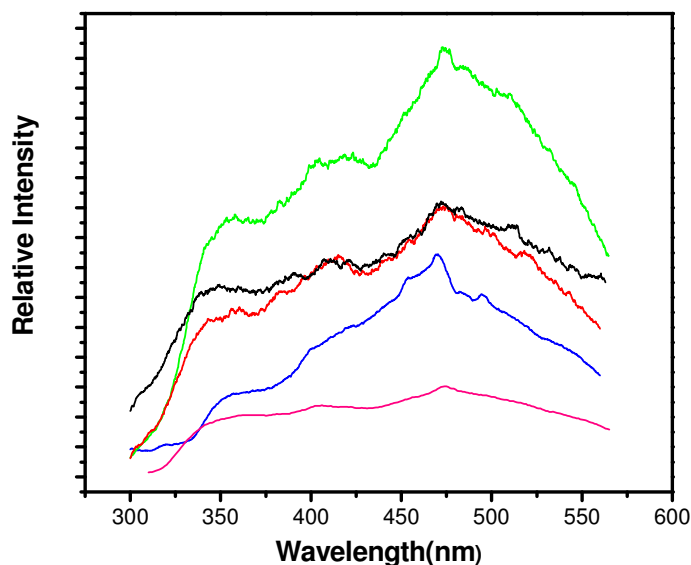


Fig. 9 Solid-state fluorescence emissions recorded at room temperature for H_2IIP (pink), **1** (red), **2** (blue), **3** (black), and **4A** (green) ($\lambda_{\text{ex}} = 290 \text{ nm}$).

Conclusions

In summary, a novel temperature-independent discrete single-walled coordination tube **1** and a two-fold interpenetrated 3D diamond network **2** were successfully obtained in the presence of bte and bpp as auxiliary ligand, respectively. In the case of using a longer spacer auxiliary ligand bbtz with more flexibility, a pair of temperature-dependent frameworks, **3** and **4**, has been synthesized. Among them, the novel SWCONT **3** was obtained at ambient temperature, while **4** was prepared under solvothermal condition at 120 °C and features an interesting two-fold 2D “embracing” (4, 4) topological network architecture. The different conformations of the auxiliary flexible ligand bbtz in **3** and **4** must be induced by different temperatures and should be responsible for the different architectures of these two frameworks. This reveals

that the more flexible is the auxiliary ligand, the assembly will be more dependent on the temperature used in synthesis. The present study also reveals that an effective strategy for the formation of novel discrete SWCONT is the use of connecting 0D elliptical dimeric nanometer-sized subunits through the rigid ligand IIP²⁻. To our best knowledge, **1** and **3** are the first discrete single-walled Cd(II)-organic tubes. Furthermore, **1-3** show *in-situ* rapid reversible dehydration-rehydration behavior just in the static air, revealing that they may be useful as potential water adsorbent or sensing materials. **1-3** and **4A** have been found to exhibit blue fluorescence in the solid state. The dehydrated **1** and **3** show selective gas adsorption to CO₂ over N₂ under high pressure. Furthermore, the dehydrated **3** may be used as adsorbent material to some protic organic solvents. Further work is in progress to prepare other novel MOFs based on H₂IIP in our laboratory.

Experimental

Materials and characterization

The starting materials, H₂IIP, bte, bpp and bbtz, were prepared according to the previously reported procedure.^{15, 27} The other reagents were purchased commercially and used without further purification. Elemental analyses (C, H and N) were carried out on a 240 C Elemental analyzer. FT-IR spectra (4000 - 400 cm⁻¹) were recorded from KBr pellets in Magna 750 FT-IR spectrophotometer. The solid state fluorescence emission spectra were recorded using an F-4500 Fluorescence spectrophotometer (Hitachi). Both the excitation and emission pass width are 5.0 nm. X-ray powder diffraction data were collected on a computer controlled Bruker D8 Advanced XRD

diffractometer operating with Cu-K $\alpha_{1/2}$ ($\lambda = 1.5418 \text{ \AA}$) at a scanning rate 0.024 °/s from 5° to 50° using a VÅNTEC solid-state detector. The diffractometer was fitted with an Anton-Parr XRK900 heating stage for variable temperature studies. Thermogravimetric analysis (TG) was taken on NETZSCH STA 409 PG/PC instrument under a stream of N₂ (10 mL/min). The sorption experiments for gases and vapors were measured with an automatic gravimetric adsorption apparatus (Magnetic Suspension Balances, Rubotherm Ltd. Germany) at 298 K. The initial outgassing process for the samples **1** and **3** was carried out under a high vacuum at 155 and 85 °C for *ca.* 4 h, respectively.

Synthesis of [Cd(IIP)(bte)(H₂O)]·H₂O (**1**)

A solution of Cd(NO₃)₂·4H₂O (15.4 mg, 0.05 mmol) was dissolved in water (4 ml) and then a solution of H₂IIP (14.6 mg, 0.05 mmol) in DMF/H₂O (10 ml, V/V = 1:1) (DMF = N,N'-Dimethylformamide) was added whilst stirring. To this solution bte (8.2 mg, 0.05 mmol) in water (4 ml) was added and then filtered. The filtrate was kept at ambient temperature for several days and pale yellow block crystals were formed.

Complex **1** can also be obtained using the following hydrothermal method. A mixture containing CdCl₂·2.5H₂O (11.4 mg, 0.05 mmol), NaOH (3.0 mg, 0.075 mmol), H₂IIP (14.6 mg, 0.05 mmol), bte (8.0 mg, 0.05 mmol) and water (6 ml) was sealed in a Teflon reactor, which was heated at 120 °C for 3 days and then it was cooled to room temperature at 5 °C·h⁻¹. Yellow block crystals were collected in a 69 % yield (based on H₂IIP). Anal. Calc. for: C₁₄H₁₅CdIN₆O₆ C, 27.90; H, 2.51; N, 13.95. Found: C, 27.99; H, 2.60; N, 13.86 %. (yield: 67 % based on H₂IIP). IR/cm⁻¹

(KBr): 3329 (m), 3162(w), 1595 (vs), 1544(vs), 1424(s), 1370(s), 1281(m), 1012(m), 926(m), 729(s), 670(s).

Synthesis of [Cd(IIP)(bpp)(H₂O)] (2)

A mixture containing CdCl₂·2.5H₂O (22.8 mg, 0.1 mmol), H₂IIP (29.2 mg, 0.1 mmol), bpp (19.8 mg, 0.1 mmol), NaOH (8.0 mg, 0.2 mmol) and water (6 ml) was sealed in a Teflon reactor, which was heated at 160 °C for 3 days, and then it was cooled to room temperature at 10 °C·h⁻¹. Colorless block crystals of 24 were collected in a 85 % yield (based on H₂IIP).

Complex 2 can also be obtained using the following typical solution method. A mixture of H₂IIP (29.0 mg, 0.1 mmol) and NaOH (4.0 mg, 0.1 mmol) was dissolved in water (10 ml) and then an aqueous solution of CdCl₂·2.5H₂O (22.0 mg, 0.1 mmol) in water (5 ml) was added whilst stirring. To this solution bpp (20.0 mg, 0.1 mmol) in N, N'-dimethylformamide (DMF) (5 ml) was added and then filtered. The filtrate was kept at ambient temperature for several days and yellow block crystals were formed. (yield: 70 % based on H₂IIP). Anal. Calc. for: C₂₁H₁₉CdIN₂O₅: C, 40.76; H, 3.09; N, 4.53. Found: C, 40.67; H, 3.12.; N, 4.71 %.

Synthesis of [Cd(IIP)(bbtz)(H₂O)]·H₂O (3)

A mixture of H₂IIP (29.0 mg, 0.1 mmol) and NaOH (4.0 mg, 0.1 mmol) was dissolved in DMF (5 ml) and then an aqueous solution of CdCl₂·2.5H₂O (22.8 mg, 0.1 mmol) in water (5 ml) was added whilst stirring. To this solution bbtz (24.0 mg, 0.1 mmol) in water (5 ml) was added and then filtered. The filtrate was kept at ambient temperature for several days and yellow block crystals were formed (yield: 59 % based on H₂IIP).

Anal. Calc. for $C_{20}H_{18}CdIN_6O_6$: C, 35.45; H, 2.68; N, 12.40. Found: C, 35.38; H, 2.80; N, 12.55 %. IR/cm⁻¹ (KBr): 3124(m), 1661(vs), 1597(m), 1545(s), 1433(s), 1369(s), 1280(w), 1131(s), 923 (w), 729(s).

Synthesis of [Cd(IIP)(bbtz)(H₂O)] (4)

A mixture containing CdCl₂·2.5H₂O (22.8 mg, 0.1 mmol), H₂IIP (29.2 mg, 0.1 mmol), bbtz (24.0 mg, 0.1 mmol), NaOH (8.0 mg, 0.2 mmol) and H₂O/EtOH (6 ml, V/V=1:1) was sealed in a Teflon reactor, which was heated at 120 °C for 3 days, and then it was cooled to room temperature at 5 °C·h⁻¹. Yellow block crystals were formed.

Complex **4** loses crystallinity in the air and changes into the pale yellow powder formulated as [Cd(IIP)(bbtz)(H₂O)_{0.5}] (**4A**) (yield: 44 % based on H₂IIP). Anal. Calc. for: $C_{20}H_{16}CdIN_6O_{4.5}$: C, 36.86; H, 2.63; N, 12.90. Found: C, 36.98; H, 2.42.; N, 12.75 %. IR/cm⁻¹ (KBr): 3381(s), 3137(w), 1606(vs), 1552(vs), 1426(vs), 1355(vs), 1284(m), 1128(s), 986(w), 789(s), 735(s), 679(m).

X-ray single-crystal structure determination

Crystallographic data were collected at 296(2) K with a Siemens SMART CCD diffractometer using graphite-monochromated (Mo-K α) radiation ($\lambda = 0.71073 \text{ \AA}$), ψ and ω scans mode. The structures were solved by direct methods and refined by Full-Matrix least-squares on F² method using SHELXL-97 program.²⁸ Intensity data were corrected for Lorenz and polarization effects and a multi-scan absorption correction was performed. Generally, the positions of C-bound H atoms were generated on idealized geometries. The H atoms of water were first located in difference Fourier maps and then kept fixed. All non-hydrogen atoms were refined

anisotropically. The contribution of the hydrogen atoms was included in the structure factor calculations. It should be noted that the “ALERT level A” problem in the checkcif/platon report of **3** indicates that the structure contains large solvent accessible voids even if both the lattice and coordinated water molecules are included, which can further be verified by thermogravimetric analyses (TG) and elemental analysis. Furthermore, from crystallographic point of view, there is nothing to do with the voids. Details of crystal data, collection and refinement are listed in Table 1.

Supplementary data

Crystallographic data have been deposited with the Cambridge Crystallographic Data Centre with CCDC reference numbers: 816409 (**1**), 816413 (**2**), 821642 (**3**) and 816412 (**4**).

Acknowledgments

We gratefully acknowledge the Natural Science Foundation of Jiangsu Province (BK2012680), the Jiangsu Government Scholarship for Overseas Studies, and the Priority Academic Program Development of Jiangsu Higher Education Institutions (PAPD).

References

- (1) (a) P. L. Llewellyn, P. Horcajada, G. Maurin, T. Devic, N. Rosenbach, S. Bourrelly, C. Serre, D. Vincent, S. Loera-Serna, Y. Filinchuk, G. Férey, *J. Am. Chem. Soc.* 2009, **131**, 13002; (b) J. An, S. Geib, N. L. Rosi, *J. Am. Chem. Soc.* 2010, **132**, 38; (c) A. G. Wong-Foy, A. J. Matzger, O. M. Yaghi, *J. Am. Chem. Soc.* 2006, **128**, 3494; (d) R. Matsuda, R. Kitaura, S. Kitagawa, Y. Kubota, R. V. Belosludov, T. C. Kobayashi, H. Sakamoto, T. Chiba, M. Takata, Y. Kawazoe, Y. Mita, *Nature*. 2005, **436**, 238; (e) L. J. Murray, M. Dinca, J. Yano, S. Chavan, S.

- Bordiga, C. M. Brown, J. R. Long, *J. Am. Chem. Soc.* 2010, **132**, 7856; (f) X. Y. Tang, A. X. Zheng, H. Shang, R. X. Yuan, H. X. Li, Z. G. Ren, J. P. Lang, *Inorg. Chem.*, 2011, **50**, 503; (g) Y. Q. Tian, Y. M. Zhao, Z. X. Chen, G. N. Zhang, L. H. Weng, D. Y. Zhao, *Chem.–Eur. J.* 2007, **13**, 4146; (h) X. H. Zhou, Y. H. Peng, X. D. Du, C. F. Wang, J. L. Zuo, X. Z. You, *Cryst. Growth Des.* 2009, **9**, 1028; (i) Z. Z. Lu, R. Zhang, Y. Z. Li, Z. J. Guo, H. G. Zheng, *J. Am. Chem. Soc.* 2011, **133**, 4172 ; (j) Y.-Q. Lan, H.-L. Jiang, S.-L. Li, Q. Xu, *Inorg. Chem.* 2012, **51**, 7484.
- (2) (a) M. Khanpour, A. Morsali, *Eur. J. Inorg. Chem.* 2010, 1567; (b) A. Morsali, M. Y. Masoumi, *Coord. Chem. Rev.* 2009, **253**, 1882; (c) Y. Chen, Z. Yang, C. X. Guo, C. Y. Ni, H. X. Li, Z. G. Ren, J. P. Lang, *CrystEngComm.*, 2011, **13**, 243; (d) D. Liu, Z. G. Ren, H. X. Li, J. P. Lang, N. Y. Li, B. F. Abrahams, *Angew. Chem. Int. Ed.*, 2010, 49, 4767; (e) B. H. Ye, M. L. Tong, X. M. Chen, *Coord. Chem. Rev.* 2005, **249**, 545; (f) Y. Y. Niu, H. G. Zheng, H. W. Hou, X. Q. Xin, *Coord. Chem. Rev.* 2004, **248**, 169; (g) J. Lee, O. K. Farha, J. Roberts, K. A. Scheidt, S. T. Nguyen, J. T. Hupp, *Chem. Soc. Rev.* 2009, **38**, 1450; (h) D. J. Tranchemontagne, J. L. Mendoza-Cortés, M. O’Keeffe, O. M. Yaghi, *Chem. Soc. Rev.* 2009, **38**, 1257; (i) G. Férey, *Chem. Soc. Rev.* 2008, **37**, 91; (j) L. J. Murray, M. Dincă, J. R. Long, *Chem. Soc. Rev.* 2009, **38**, 1294; (k) L. Du, Z. Lu, K. Zheng, J. Wang, X. Zheng, Y. Pan, X. You, and J. Bai, *J. Am. Chem. Soc.* 2013, **135**, 562.
- (3) (a) A. Datcu, N. Roques, V. Jubera, D. MasPOCH, X. Fontrodona, K. Wurst, I. Imaz, G. Mouchaham, J.-P. Sutter, C. Rovira, J. Veciana *Chem.–Eur. J.* 2012, **18**, 152; (b) P. Kanoo, A. C. Ghosh, S. T. Cyriac and T. K. Maji *Chem.–Eur. J.* 2012, **18**, 237; (c) T. Jacobs and M. J. Hardie *Chem.–Eur. J.* 2012, **18**, 267. (d) H. Reinsch, M. A. van der Veen, B. Gil, B. Marszalek, T. Verbiest, D. de Vos, N. Stock, *Chem. Mater.* 2013, **25**, 17.
- (4) J. M. Lehn.; *Supramolecular Chemistry: Concepts and Perspectives*; VCH: New York, 1995.
- (5) (a) J. S. Seo, D. Whang, H. Lee, S. I. Jun, J. Oh, Y. J. Jeon, K. Kim, *Nature.* 2000, **404**, 982; (b) M. Eddaoudi, J. Kim, N. Rosi, D. Vodak, J. Wachter, M. O’Keeffe, O. M. Yaghi, *Science.* 2002, **295**, 469; (c) L. Pan, H. Liu, X. Lei, X. Huang, D. H.

- Olson, N. J. Turro, J. Li, *Angew. Chem. Int. Ed.* 2003, **42**, 542.
- (6) (a) Z. Su, K. Cai, J. Fan, S. S. Chen, M. S. Chen, W. Y. Sun, *CrystEngComm*. 2010, **12**, 100; (b) G. X. Liu, Y.Q. Huang, Q. Chu, T. Okamura, W. Y. Sun, H. Liang, N. Ueyama, *Cryst. Growth Des.* 2008, **8**, 3233; (c) S. S. Chen, M. Chen, S. Takamizawa, P. Wang, G. C. Lv and W. Y. Sun, *Chem. Commun.*, 2011, **47**, 4902; (d) K. L. Zhang, Y. Chang, C. T. Hou, G. W. Diao, R. Wu, S. W. Ng, *CrystEngComm*. 2010, **12**, 1194.
- (7) (a) B. Wang, A. P. Côté, H. Furukawa, M. O'Keeffe, O. M. Yaghi, *Nature*. 2008, **453**, 207; (b) E. Tang, Y. M. Dai, J. Zhang, Z. J. Li, Y. G. Yao, J. Zhang, X. D. Huang, *Inorg. Chem.* 2006, **45**, 6276; (c) F. Luo, S. R. Batten, Y. X. Che, J. M. Zheng, *Chem. Eur. J.* 2007, **13**, 4948; (d) F. Yu, X. J. Kong, Y. Y. Zheng, Y. P. Ren, L. S. Long, R. B. Huang, L. S. Zheng, *Dalton Trans.* 2009, 9503.
- (8) V. Iancu, A. Deshpande, S.-W. Hia, *Nano Lett.* 2006, **6**, 820.
- (9) (a) S. Mosaoka, D. Tanaka, Y. Nakanishi, S. Kitagawa, *Angew. Chem. Int. Ed.* 2004, **43**, 2530; (b) X.-S. Wang, S. Ma, P. M. Forster, D. Yuan, J. Eckert, J. J. Lopez, B. J. Murphy, J. B. Praise, H.-C. Zhou, *Angew. Chem., Int. Ed.* 2008, **47**, 7263.
- (10) C. Janiak, L. Uehlin, H.-P. Wu, P. Klêufers, H. Piotrowski, T. G. Scharmann, *J. Chem. Soc. Dalton Trans.* 1999, 3121.
- (11) S. Lijima, *Nature* 1991, **354**, 56.
- (12) (a) Y. Cui, S. J. Lee, W. B. Lin. *J. Am. Chem. Soc.* 2003, **125**, 6014; (b) X. L. Wang, C. Qin, E. B. Wang, L. Xu, Z. M. Su, C. W. Hu, *Angew. Chem., Int. Ed.* 2004, **43**, 5036; (c) M. C. Hong, Y. J. Zhao, W. P. Su, *Angew. Chem., Int. Ed.* 2000, **39**, 2468; (d) O. S. Jung, Y. J. Kim, K. M. Kim, Y. A. Lee, *J. Am. Chem. Soc.* 2002, **124**, 7906; (e) P. Jensen, S. R. Batten, B. Moubaraki, K. S. Murray, *Chem. Commun.* 2000, 793; (f) L. J. Murray, M. Dinca, J. R. Long, *Chem. Soc. Rev.* 2009, **38**, 1294; (g) J. Lee, O. K. Farha, J. Roberts, K. A. Scheidt, S. T. Nguyen, J. T. Hupp, *Chem. Soc. Rev.* 2009, **38**, 1450; (h) A. C. McKinlay, R. E. Morris, P. Horcajada, G. Férey, R. Gref, P. Couvreur, C. Serre, *Angew. Chem., Int. Ed.* 2010, **49**, 6260.

- (13) (a) F. N. Dai, H. Y. He and D. F. Sun, *J. Am. Chem. Soc.*, 2008, **130**, 14064; (b) F. N. Dai, H. Y. He and D. F. Sun, *Inorg. Chem.* 2009, **48**, 4613; (c) X. L. Wang, C. Qin, E. B. Wang, Y. G. Li, Z. M. Su, L. Xu and L. Carlucci, *Angew. Chem., Int. Ed.*, 2005, **44**, 5824; (d) M. Aoyagi, K. Biradha, M. Fujita, *J. Am. Chem. Soc.* 1999, **121**, 7457; (e) T. Yamaguchi, S. Tashiro, M. Tominaga, M. Kawano, T. Ozeki, M. Fujita, *J. Am. Chem. Soc.* 2004, **126**, 10818; (f) S. Tashiro, M. Tominaga, T. Kusukawa, M. Kawano, S. Sakamoto, K. Yamaguchi, M. Fujita, *Angew. Chem., Int. Ed.* 2003, **42**, 3267; (g) C. Y. Su, M. D. Smith, H. Loye, *Angew. Chem., Int. Ed.* 2003, **42**, 4085.
- (14) (a) J. Fan, H. F. Zhu, T. A. Okamura, W. Y. Sun, W. X. Tang, N. Ueyama, *Inorg. Chem.* 2003, **42**, 158; (b) F. Chang, Z. M. Wang, H. L. Sun, S. Gao, G. H. Wen, X. X. Zhang, *J. Chem. Soc., Dalton Trans.*, 2005, 2976; (c) A. M. Madalan, C. Paraschiv, J. P. Sutter, M. Schmidtman, A. Müller, M. Andruh, *Cryst. Growth Des.* 2005, **5**, 707; (d) Y. B. Dong, Y. Y. Jiang, J. Li, J. P. Ma, F. L. Liu, *J. Am. Chem. Soc.* 2007, **129**, 4520; (e) Y. J. Dong, Y. Y. Jiang, J. P. Ma, F. L. Liu, J. Li, B. Tang, R. Q. Huang and S. R. Batten, *J. Am. Chem. Soc.*, 2007, **129**, 4520; (f) G. Z. Yuan, C. F. Zhu, Y. Liu, W. M. Xuan and Y. Cui, *J. Am. Chem. Soc.*, 2009, **131**, 10452; (g) J. Xia, W. Shi, X. Y. Chen, H. S. Wang, P. Cheng, D. Z. Liao and S. P. Yan, *Dalton Trans.*, 2007, 2373; (h) P. Jensen, S. R. Batten, B. Moubaraki and K. S. Murray, *Chem. Commun.*, 2000, 793; (i) X. Y. Cao, J. Zhang, J. K. Cheng, Y. Kang and Y. G. Yao, *CrystEngComm.*, 2004, **6**, 315; (j) S. B. Ren, X. L. Yang, J. Zhang, Y. Z. Li, Y. X. Zheng, H. B. Du and X. Z. You, *CrystEngComm.*, 2009, **11**, 246; (k) H. Kitagawa and K. Otsubo, *Nat. Mater.* 2011, **10**, 291.
- (15) K. -L. Zhang, C. T. Hou, J.-J. Song, Y. Deng, L. Li, S. W. Ng, G.-W. Diao, *CrystEngComm*, 2012, **14**, 590.
- (16) (a) J. Fan, W.-Y. Sun, T. Okamura, Y.-Q. Zheng, B. Sui, W.-X. Tang and N. Ueyama *Cryst. Growth Des.* 2004, **4**, 579; (b) K. Rissanen, *CrystEngComm.* 2008, **10**, 1107; (c) L. Brammer, G. M. Espallargas and S. Libri, *CrystEngComm.* 2008, **10**, 1712.
- (17) X.-Q. Liang, D.-P. Li, X.-H. Zhou, Y. Sui, Y.-Z. Li, J.-L. Zuo and X.-Z. You

- Cryst. Growth Des.* 2009, **9**, 4872.
- (18) Y.-F. Peng, H.-Y. Ge, B.-Z. Li, B.-L. Li and Y. Zhang, *Cryst. Growth Des.* 2006, **6**, 994.
- (19) A. L. Spek, *PLATON, A Multipurpose Crystallographic Tool*, Utrecht University, Utrecht, The Netherlands, 2002.
- (20) D. Eisenberg, W. Kauzmann, *The Structure and Properties of Water*. Oxford University Press: Oxford, 1969.
- (21) K. Nakamoto, *Infrared and Raman Spectra of Inorganic and Coordination Compounds*, 4th edn., Wiley, New York. 1986, 231.
- (22) G. Férey, C. Serre, *Chem. Soc. Rev.* 2009, **38**, 1380.
- (23) (a) S. Coriani, A. Halkier, A. Rizzo and K. Ruud, *Chem. Phys. Lett.*, 2000, **326**, 269; (b) L. Du, Z. Lu, K. Zheng, J. Wang, X. Zheng, Y. Pan, X. You, J. Bai, *J. Am. Chem. Soc.* 2013, **135**, 562.
- (24) S. T. Wang, Y. Hou, E. B. Wang, Y. G. Li, L. Xu, J. Peng, S. X. Liu, C. W. Hu, *New J. Chem.* 2003, **27**, 1144.
- (25) S. J. A. Pope, B. J. Coe, S. Faulkner, E. V. Bichenkova, X. Yu, K. T. Douglas, *J. Am. Chem. Soc.* 2004, **126**, 9490.
- (26) (a) S. L. Zheng, J. M. Yang, X. L. Yu, X. M. Chen and W. T. Wong, *Inorg. Chem.* 2004, **43**, 830; (b) S. L. Zheng, M. L. Tong, S. D. Tan, Y. Wang, J. X. Shi, Y. X. Tong, H. K. Lee and X. M. Chen, *Organometallics*. 2001, **20**, 5319.
- (27) (a) J. Torres, J. L. Lavandera, P. Cabildo, R. M. Claramunt, J. Elguero, *J. Heterocycl. Chem.* 1988, **25**, 771; (b) Y. F. Peng, B. Z. Li, J. H. Zhou, B. L. Li, Y. Zhang, *Chin. J. Struct. Chem.* 2004, **23**, 985.
- (28) G. M. Sheldrick, *SHELXL 97. Programs for Crystal Structure Analysis (Release 97-2)*, 1997, University of Göttingen, Germany.

Table 1. Crystallographic data and structure refinement details for **1-4**.

Complex	1	2	3	4
Empirical formula	C ₁₄ H ₁₅ CdIN ₆ O ₆	C ₂₁ H ₁₉ CdIN ₂ O ₅	C ₂₀ H ₁₈ CdIN ₆ O ₆	C ₂₀ H ₁₇ CdIN ₆ O ₅
Formula weight	602.62	618.68	677.70	660.70
Temperature	296(2)	296(2)	296(2)	296(2)
Wavelength/ Å	0.71073	0.71073	0.71073	0.71073
Crystal system	Monoclinic	Monoclinic	Triclinic	Monoclinic
Space group	<i>C2/c</i>	<i>C2/C</i>	<i>P-1</i>	<i>P2₁/c</i>
<i>a</i> /Å	21.071(2)	14.4247(16)	10.3338(16)	8.9822(8)
<i>b</i> /Å	10.4609(11)	19.279(2)	10.7432(16)	26.469(2)
<i>c</i> /Å	20.255(2)	16.6099(19)	14.173(2)	11.0259(7)
α /°	90	90	71.448(2)	90□
β /°	120.0380(10)	102.928(2)	86.073(2)	102.3130(10)
γ /°	90	90	73.862(2)	90
<i>V</i> / Å ³	3865.0(7)	4502.0(9)	1432.6(4)	2287.1(3)
<i>Z</i>	8	8	2	4
<i>D_c</i> / Mg m ⁻³	2.071	1.826	1.571	1.919
Absorption coeff /mm ⁻¹	2.722	2.375	1.880	2.349
<i>F</i> (000)	2320	2400	658	1280
θ range for data collection /°	2.23 to 27.63	1.79 to 27.51	2.05 to 25.00	1.54 to 27.53
Index ranges	-27≤ <i>h</i> ≤27 -12≤ <i>k</i> ≤13 -26≤ <i>l</i> ≤26	-18≤ <i>h</i> ≤18 -23≤ <i>k</i> ≤24 -21≤ <i>l</i> ≤20	-11≤ <i>h</i> ≤12 -12≤ <i>k</i> ≤12 -16≤ <i>l</i> ≤16	-11≤ <i>h</i> ≤10 -34≤ <i>k</i> ≤34 -14≤ <i>l</i> ≤14
Reflections collected	16513	19537	10485	19945
Unique(<i>R_{int}</i>)	4488 [<i>R</i> (int)= 0.0318]	5168 (<i>R_{int}</i> =0.0370)	4990 [<i>R</i> (int)=0.0332]	5233 [<i>R</i> (int)= 0.0388]
Completeness	99.5 %	99.7 %	99.0 %	99.1 %
Max. and min. transmission	0.591 and 0.502	0.700 and 0.613	0.754 and 0.575	0.640 and 0.528
Goof on <i>F</i> ²	1.030	1.028	0.997	1.044
Final <i>R</i> indices [<i>I</i> >2σ(<i>I</i>)]	<i>R</i> ₁ = 0.0271 <i>wR</i> ₂ = 0.0604	<i>R</i> ₁ = 0.0428 <i>wR</i> ₂ = 0.0993	<i>R</i> ₁ = 0.0624 <i>wR</i> ₂ = 0.2082	<i>R</i> ₁ = 0.0293 <i>wR</i> ₂ = 0.0645
<i>R</i> indices (all data)	<i>R</i> ₁ = 0.0393 <i>wR</i> ₂ = 0.0671	<i>R</i> ₁ = 0.0669 <i>wR</i> ₂ = 0.1117	<i>R</i> ₁ = 0.0900 <i>wR</i> ₂ = 0.2308	<i>R</i> ₁ = 0.0388 <i>wR</i> ₂ = 0.0704
Largest diff. Peak and hole / e Å ⁻³	0.605 and -0.698	1.432 and -1.560	2.472 and -1.065	0.645 and -0.594

Table 2. Selected bond lengths [Å] and angles [°] for 1-3.

Complex 1			
Cd(1)-O(1)	2.286(2)	Cd(1)-O(1W)	2.313(2)
Cd(1)-N(6)#1	2.288(3)	Cd(1)-N(1)	2.343(3)
Cd(1)-O(4)#2	2.303(2)	Cd(1)-O(3)#2	2.628(2)
O(1)-Cd(1)-N(6) #1	134.14(8)	O(4) #2-Cd(1)-N(1)	85.44(9)
O(1)-Cd(1)-O(4) #2	91.97(8)	O(1W)-Cd(1) -N(1)	173.81(8)
N(6)#1-Cd(1)-O(4) #2	133.84(8)	O(1)-Cd(1)-O(3) #2	144.43(7)
O(1)-Cd(1) -O(1W)	86.71(8)	N(6) #1-Cd(1)- O(3) #2	81.42(8)
N(6) #1-Cd(1)-O(1W)	91.36(9)	O(4) #2-Cd(1)-O(3)#2	52.56(7)
O(4) #2-Cd(1)-O(1W)	89.05(8)	O(1W)-Cd(1) -O(3) #2	94.36(7)
O(1)-Cd(1) -N(1)	90.66(9)	N(1)-Cd(1)-O(3)#2	84.52(8)
N(6) #1-Cd(1)-N(1)	94.49(9)		
Complex 2			
Cd(1)-O(3)#1	2.225(4)	Cd(1)-O(1)	2.240(3)
Cd(1)-N(1)	2.289(4)	Cd(1)-O(1W)	2.361(3)
Cd(1)-N(2)#2	2.382(4)	Cd(1)-O(2)	2.648(4)
O(3)#1-Cd(1)-O(1)	130.94(15)	O(3)#1-Cd(1)-N(1)	89.84(15)
O(1)-Cd(1)-N(1)	139.09(14)	O(3)#1-Cd(1)-O(1W)	80.56(15)
O(1)-Cd(1)-O(1W)	88.85(13)	N(1)-Cd(1)-O(1W)	96.20(13)
O(3)#1-Cd(1)-N(2)#2	91.78(15)	O(1)-Cd(1)-N(2)#2	88.79(14)
N(1)-Cd(1)-N(2)#2	93.62(14)	O(1W)-Cd(1)-N(2)#2	167.50(13)
O(3)#1-Cd(1)-O(2)	175.76(13)	O(1)-Cd(1)-O(2)	52.65(12)
N(1)-Cd(1)-O(2)	86.46(13)	O(1W)-Cd(1)-O(2)	97.77(13)
N(2)#2-Cd(1)-O(2)	90.53(13)		
Complex 3			
Cd(1)-O(1)	2.279(6)	Cd(1)-O(2W)	2.309(7)
Cd(1)-N(6)#1	2.306(8)	Cd(1)-N(1)	2.326(9)
Cd(1)-O(3)#2	2.323(6)	Cd(1)-O(4)#2	2.574(6)
O(1)-Cd(1)-N(6) #1	133.7(3)	O(2W)-Cd(1)-O(3) #2	90.2(3)
O(1)-Cd(1)-O(2W)	85.8(2)	N(1)-Cd(1)-O(3) #2	86.0(3)
N(6)#1-Cd(1)-O(2W)	90.1(3)	O(1)-Cd(1)-O(4) #2	140.5(2)
O(1)-Cd(1)-N(1)	91.9(3)	N(6)#1-Cd(1)-O(4) #2	85.2(2)
N(6)#1-Cd(1)-N(1)	94.2(3)	O(2W)-Cd(1)-O(4) #2	88.1(2)
O(2W)-Cd(1)-N(1)	175.6(3)	N(1)-Cd(1)-O(4) #2	91.4(3)
O(1)-Cd(1)-O(3)#2	87.5(2)	O(3)#2-Cd(1)-O(4) #2	53.5(2)
N(6) #1-Cd(1)-O(3) #2	138.7(2)		
Complex 4			

Cd(1)-O(4)#1	2.253(2)	Cd(1)-O(1W)	2.322(3)
Cd(1)-N(1)	2.259(3)	Cd(1)-N(6)#2	2.375(3)
Cd(1)-O(1)	2.293(2)	Cd(1)-O(2)	2.530(2)
O(4) #1-Cd(1)-N(1)	133.84(9)	O(1)-Cd(1)-N(6) #2	85.65(10)
O(4) #1-Cd(1)-O(1)	88.95(9)	O(1W)-Cd(1)-N(6) #2	177.53(10)
N(1)-Cd(1) -O(1)	137.21(9)	O(4) #1-Cd(1)-O(2)	142.08(8)
O(4) #1-Cd(1)-O(1W)	88.92(10)	N(1)-Cd(1)-O(2)	83.63(9)
N(1)-Cd(1) -O(1W)	87.37(11)	O(1)-Cd(1)-O(2)	53.88(8)
O(1)-Cd(1) -O(1W)	94.84(11)	O(1W)-Cd(1)-O(2)	100.32(10)
O(4)#1-Cd(1)-N(6) #2	88.67(10)	N(6)#2-Cd(1)-O(2)	81.93(11)
N(1)-Cd(1)-N(6) #2	93.92(11)		

Symmetry transformations: #1 $-x+2, -y, -z+1$ #2 $x, y-1, z$ #3 $x, y+1, z$ for **1**; #1 $1-x, -y, 1-z$ #2 $x-1, y, z$ for **3**; #1 $x-1, y, z-1$ #2 $-x+2, y+1/2, -z+1/2$ for **4**.

Table 3 Hydrogen bonds for 1-3.

D-H...A	d(D-H)	d(H...A)	d(D...A)	<DHA	Symmetry of A
Complex 1					
O1W -- H1WA ... O3	0.8400	1.8600	2.689(3)	168.00	$5/2-x, 1/2-y, 1-z$
O1W -- H1WB ... O2W	0.8500	1.9000	2.735(4)	170.00	$1/2+x, -1/2+y, z$
O2W -- H2WA ... N2	0.8400	2.3400	3.130(5)	157.00	$x, 1+y, z$
O2W -- H2WB ... O2	0.8400	1.9100	2.755(4)	178.00	$2-x, 1-y, 1-z$
Complex 2					
O1W -- H1WB ... O4	0.8500	1.8600	2.688(5)	164.00	$2-x, y, -1/2-z$
O1W -- H1WA ... O1	0.8500	2.1500	2.901(5)	148.00	$2-x, 1-y, -z$
Complex 3					
O1W -- H1WA ... O2	0.8500	2.0600	2.725(16)	134.00	$2-x, -y, 1-z$
O2W -- H2WB ... O1W	0.8500	1.9000	2.705(13)	156.00	$x, -1+y, 1+z$
O2W -- H2WA ... O4	0.8500	2.2500	2.677(10)	111.00	$2-x, -1-y, 2-z$
Complex 4					
O1W -- H1WA ... O3	0.8500	1.9100	2.746(4)	165.00	$-1+x, 3/2-y, -1/2+z$
O1W -- H1WB ... N5	0.8500	2.1500	2.848(6)	139.00	$1-x, 1/2+y, 1/2-z$

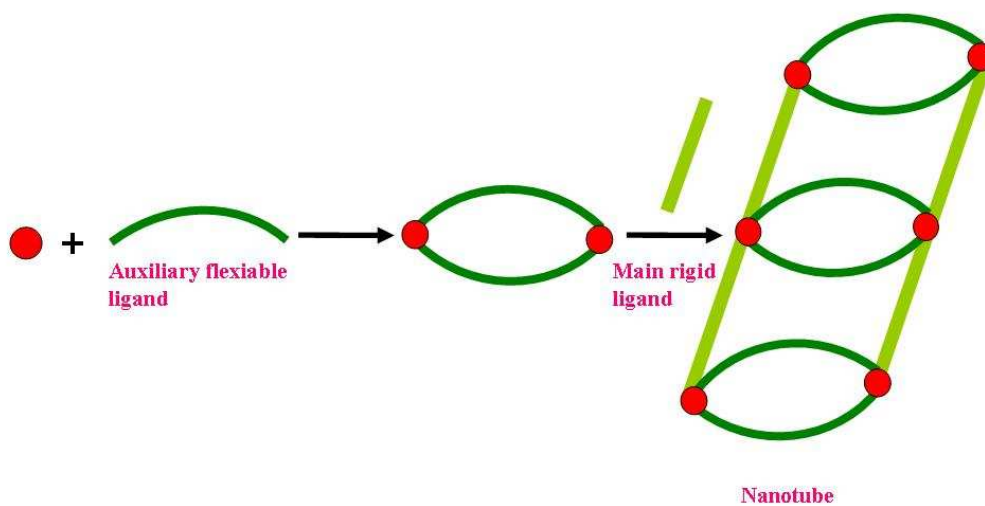
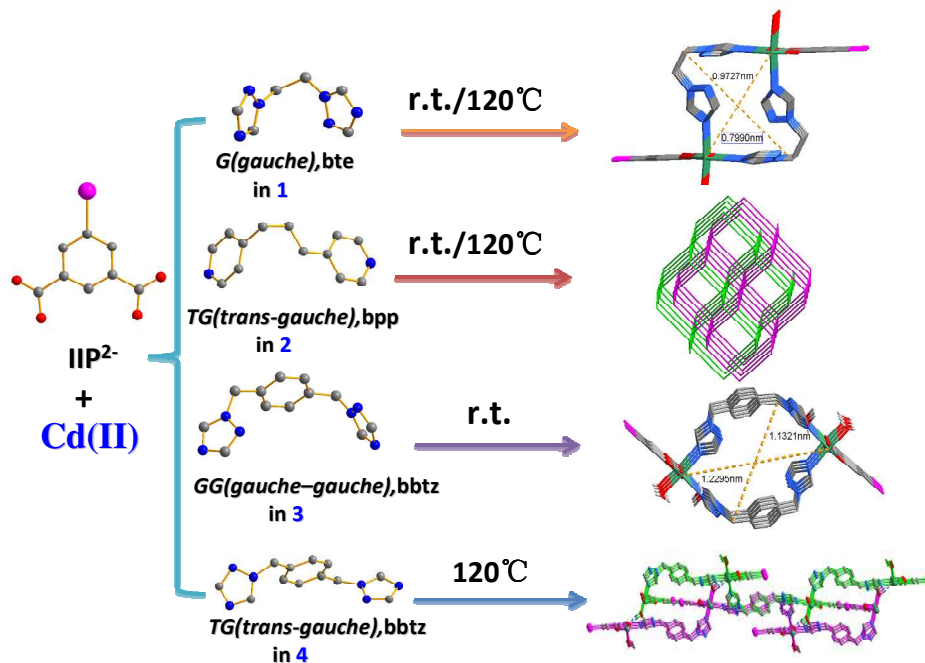
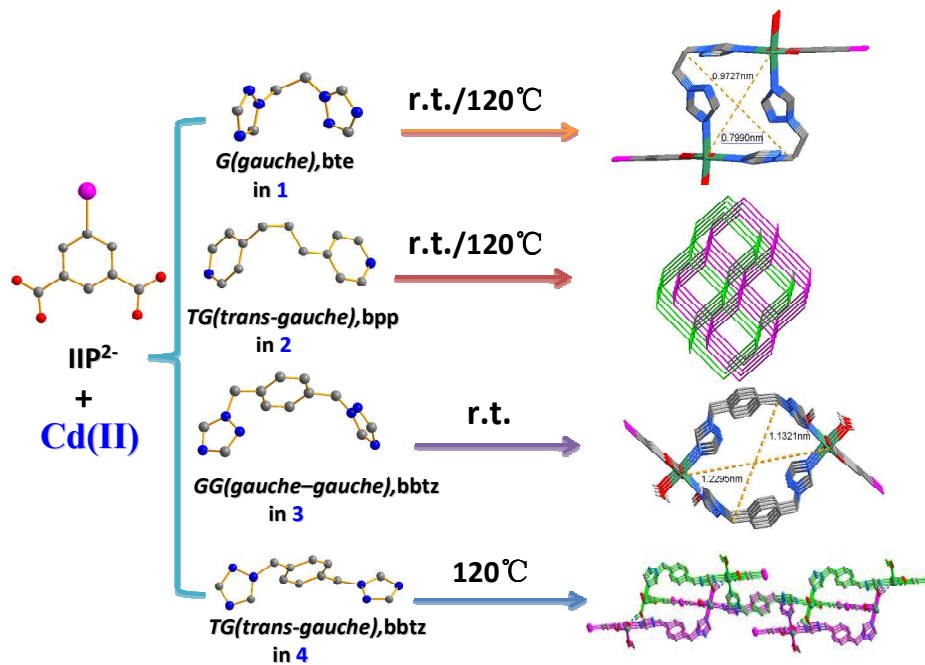


Chart 1 Construction of the discrete single-walled Cd(II)-organic nanotube.



Scheme 1. Simplified representation of the syntheses and crystalline architectures of 1-4, also showing the conformations of the auxiliary flexible ligands bte, bpp and bbtz in these four MOFs.



Simplified representation of the syntheses and crystalline architectures of 1-4.